

Dissertation zur Erlangung des Doktorgrades
der Fakultät für Chemie und Pharmazie
der Ludwig-Maximilians Universität München



**Structural and functional analysis of the
 $\text{Ca}_v1.4$ L-type calcium channel
from mouse retina**

Ludwig Baumann

aus

Eichendorf

2006

Erklärung

Diese Dissertation wurde im Sinne von § 13 Abs. 3 bzw. 4 der Promotionsordnung vom 29. Januar 1998 von Prof. Dr. Martin Biel betreut.

Ehrenwörtliche Versicherung

Diese Dissertation wurde selbständig, ohne unerlaubte Hilfe erarbeitet.

München, den 25.04.2006

München, den 25.04.2006

Ludwig Baumann

| | |
|-----------------------------|----------------------|
| Dissertation eingereicht am | 27.04.2006 |
| 1. Gutachter: | Prof. Dr. M. Biel |
| 2. Gutachter: | Prof. Dr. A. Pfeifer |
| Mündliche Prüfung am | 18.05.2006 |

CONTENTS

| | |
|--|-----------|
| 1 INTRODUCTION | 8 |
| 1.1 Nomenclature and structure of voltage-gated calcium channels | 8 |
| 1.2 L-type calcium channels | 10 |
| 1.3 Structure and regulation of the $\alpha 1$ subunit | 11 |
| <i>1.3.1 Pharmacological regulation of L-type calcium channels</i> | <i>12</i> |
| <i>1.3.2 Regulation by voltage and Ca^{2+} ions</i> | <i>12</i> |
| 1.4 Physiological impact of $Ca_v1.4\alpha 1$ | 14 |
| 1.5 Purpose of the study | 16 |
| | |
| 2 MATERIALS AND METHODS | 17 |
| | |
| 2.1 Calcium channel constructs | 17 |
| <i>2.1.1 Constructs for electrophysiology</i> | <i>17</i> |
| <i>2.1.1.1 Construction of $Ca_v1.4\alpha 1$ mutants</i> | <i>17</i> |
| <i>2.1.1.2 Construction of $Ca_v1.2b\alpha 1 / Ca_v1.4\alpha 1$ chimeric channels</i> | <i>18</i> |
| <i>2.1.2 Constructs for GST pull-down</i> | <i>18</i> |
| <i>2.1.3 Constructs for coimmunoprecipitation</i> | <i>19</i> |
| | |
| 2.2 Amplification and purification of DNA | 20 |
| <i>2.2.1 Transformation of competent <i>E. coli</i></i> | <i>20</i> |
| <i>2.2.2 Mini-Prep DNA isolation from <i>E. coli</i></i> | <i>21</i> |
| <i>2.2.3 Maxi-Prep DNA isolation from <i>E. coli</i></i> | <i>21</i> |
| | |
| 2.3 Cell culture | 21 |

| | | |
|--------------|---|-----------|
| 2.3.1 | <i>Culture of HEK 293 cells</i> | 21 |
| 2.3.2 | <i>Transient transfection of HEK 293 cells for coimmunoprecipitation</i> | 22 |
| 2.3.3 | <i>Transient transfection of HEK 293 cells for electrophysiology</i> | 22 |
| 2.4 | Analysis of proteins | 23 |
| 2.4.1 | <i>GST pull-down assay</i> | 23 |
| 2.4.1.1 | <i>Purification of GST fusion proteins expressed in E. coli</i> | 23 |
| 2.4.1.2 | <i>Expression of 6xHis/Flag tagged ICDI peptide in E. coli</i> | 23 |
| 2.4.1.3 | <i>Measurement of GST fusion protein concentration</i> | 24 |
| 2.4.1.4 | <i>Measurement of overall protein concentration</i> | 24 |
| 2.4.1.5 | <i>Interaction with calmodulin</i> | 24 |
| 2.4.1.6 | <i>Interaction with ICDI</i> | 24 |
| 2.4.2 | <i>Coimmunoprecipitation</i> | 25 |
| 2.4.2.1 | <i>Purification of proteins expressed in HEK 293 cells</i> | 25 |
| 2.4.2.2 | <i>Quantification of proteins</i> | 25 |
| 2.4.2.3 | <i>Coimmunoprecipitation of proteins</i> | 25 |
| 2.4.3 | <i>Western blot analysis</i> | 26 |
| 2.4.3.1 | <i>SDS-polyacrylamid gel electrophoresis (SDS-PAGE)</i> | 26 |
| 2.4.3.2 | <i>Immunological detection of proteins</i> | 27 |
| 2.5 | Electrophysiology | 29 |
| 2.5.1 | <i>Performance</i> | 29 |
| 2.5.2 | <i>Protocols</i> | 30 |
| 2.5.3 | <i>Data Analysis</i> | 30 |
| 3 | RESULTS | 33 |
| 3.1 | Functional characterization of Ca_v1.4α1 | 33 |
| 3.1.1 | <i>Electrophysiological properties of wild type Cav1.4α1</i> | 33 |
| 3.1.2 | <i>Pharmacological properties of wild type Ca_v1.4α1</i> | 39 |

| | |
|---|-----------|
| 3.2 The lack of calcium dependent inactivation (CDI) | 40 |
| <i>3.2.1 Calmodulin binding of $Ca_v1.4\alpha1$</i> | <i>40</i> |
| <i>3.2.2 Identification of an inhibitory channel domain</i> | <i>42</i> |
| <i>3.2.3 Interaction of ICDI and $Ca_v1.4\alpha1$</i> | <i>43</i> |
| <i>3.2.4 Abolishing CDI in $Ca_v1.2$ channels</i> | <i>45</i> |
| | |
| 4 DISCUSSION | 48 |
| | |
| 4.1 Functional characterization of $Ca_v1.4\alpha1$ | 48 |
| <i>4.1.1 Electrophysiological properties of $Ca_v1.4\alpha1$</i> | <i>48</i> |
| <i>4.1.2 Pharmacological profile of $Ca_v1.4\alpha1$</i> | <i>49</i> |
| | |
| 4.2 Proposed mechanism for block of CDI in $Ca_v1.4$ channels | 50 |
| | |
| 4.3 Physiological function of $Ca_v1.4$ calcium channels | 53 |
| | |
| 5 SUMMARY | 55 |
| | |
| 6 APPENDIX | 57 |
| | |
| 6.1 Sequence of $Ca_v1.4\alpha1$ cloned from mouse retinal cDNA | 57 |
| | |
| 6.2 Alignment | 64 |
| | |
| 6.3 Primers | 65 |
| | |
| 7 REFERENCES | 66 |
| | |
| 8 PUBLICATIONS | 72 |

9 ACKNOWLEDGEMENTS..... 73

10 CURRICULUM VITAE..... 74

ABBREVIATIONS

| | |
|----------|--|
| ANOVA: | Analysis of variance |
| CDI: | Calcium dependent inactivation |
| CNG: | Cyclic-nucleotide-gated |
| cDNA: | Cyclic deoxyribonucleic acid |
| CSNB: | Congenital stationary nightblindness |
| DMEM: | Dulbecco's modified eagle medium |
| DHP: | Dihydropyridine |
| DNA: | Desoxyribonucleic acid |
| DTT: | 1,4-Dithiothreitol |
| E. coli: | Escherichia coli |
| EDTA: | Ethylenediaminetetraacetic acid |
| EGFP | Enhanced green fluorescent protein |
| EGTA | Ethylene glycol bis(β-aminoethylether) tetraacetic acid |
| FBS: | Fetal bovine serum |
| GST: | Glutathione-S-transferase |
| HEK: | Human embryonal kidney |
| HEPES: | 2-[4-(2-Hydroxyethyl)-1-piperazinyl]-ethanesulfonic acid |
| HVA: | High voltage-activated |
| ICDI: | Inhibitor of calcium dependent inactivation |
| LB: | Luria-Bertani |
| LTCC: | L-type calcium channel |
| LVA: | Low voltage-activated |
| PAGE: | Polyacrylamide gel electrophoresis |
| PBS: | Phosphate buffered saline |
| PO: | Pore occluder |
| PVDF: | Polyvinylidene difluoride |
| SDS: | Sodium dodecyl sulfate |
| SEM: | Standard error of the mean |
| TEA: | Tetraethylammonium chloride |
| TEMED: | N,N,N',N'-Tetramethylethylenediamine |
| TBS: | Tris buffered saline |
| Tris: | Tris(hydroxymethyl)aminomethane |
| VDI: | Voltage dependent inactivation |

1 INTRODUCTION

Voltage-gated calcium channels are members of a gene superfamily of transmembrane ion channel proteins which also includes voltage-gated sodium and potassium channels. They mediate Ca^{2+} influx into the cell along an electrochemical gradient in response to changes in the membrane potential. Owing to this property voltage-gated calcium channels couple electrical signaling with numerous physiological events like muscle contraction, secretion, gene expression, cell division or neurotransmission^{1,2}.

1.1 Nomenclature and structure of voltage-gated calcium channels

The calcium channels are protein complexes consisting of four to five subunits (Figure 1-1). The largest peptide of the complex is the α_1 subunit with about 190-250kDa. This protein contains the channel pore, the voltage sensor and the gating machinery. The β subunit is localized at the intracellular face of the channel complex. The transmembrane δ subunit and the extracellular α_2 subunit are linked by disulfid-bonds forming the $\alpha_2\delta$ subunit complex¹. The voltage-gated calcium channel of skeletal muscle contains an additional γ subunit³, which is also a transmembrane protein.

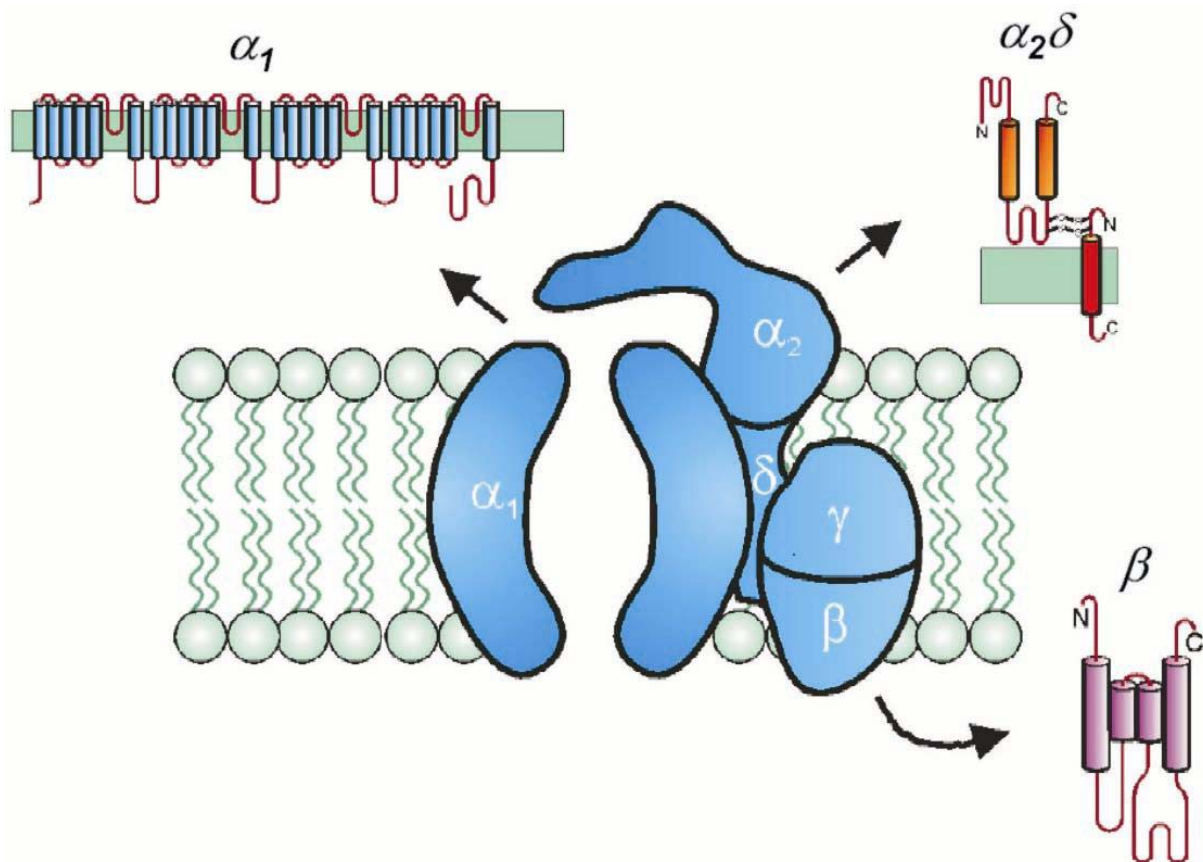


Figure 1-1 Schematic representation of a voltage-gated calcium channel subunit complex.

The principal pharmacological and electrophysiological properties of voltage-gated calcium channels are determined by the respective α_1 subunits. By contrast, β , $\alpha_2\delta$ and γ subunits are modulatory proteins which fine-tune the basic properties of the channel complex⁴.

α_1 subunits are divided into two groups, the high voltage-activated (HVA) and the low voltage-activated (LVA) channels, according to their activation threshold (Figure 1-2). With respect to their pharmacological properties the HVA calcium channels can be distinguished further on into subclasses⁵. The first class, the so-called L-type calcium channels (LTCCs) ($Ca_v1.1$ - $Ca_v1.4$), produces a long lasting ("L") current which is sensitive to organic LTCC blockers including dihydropyridines, phenylalkylamines and benzothiazepines. P/Q-type, N-type and R-type channels ($Ca_v2.1$ - $Ca_v2.3$) are also high voltage-activated but they are only weakly affected by the L-type channel blockers. These channels typically can be blocked by specific polypeptide toxins from snail and spider venoms¹.

The LVA calcium channels, which need only weak depolarizations for activation, produce the so-called T-type current ($Ca_v3.1$ - $Ca_v3.3$). It is a transient current ("T"), resistant to subtype-specific channel blockers the other calcium channels are sensitive to.

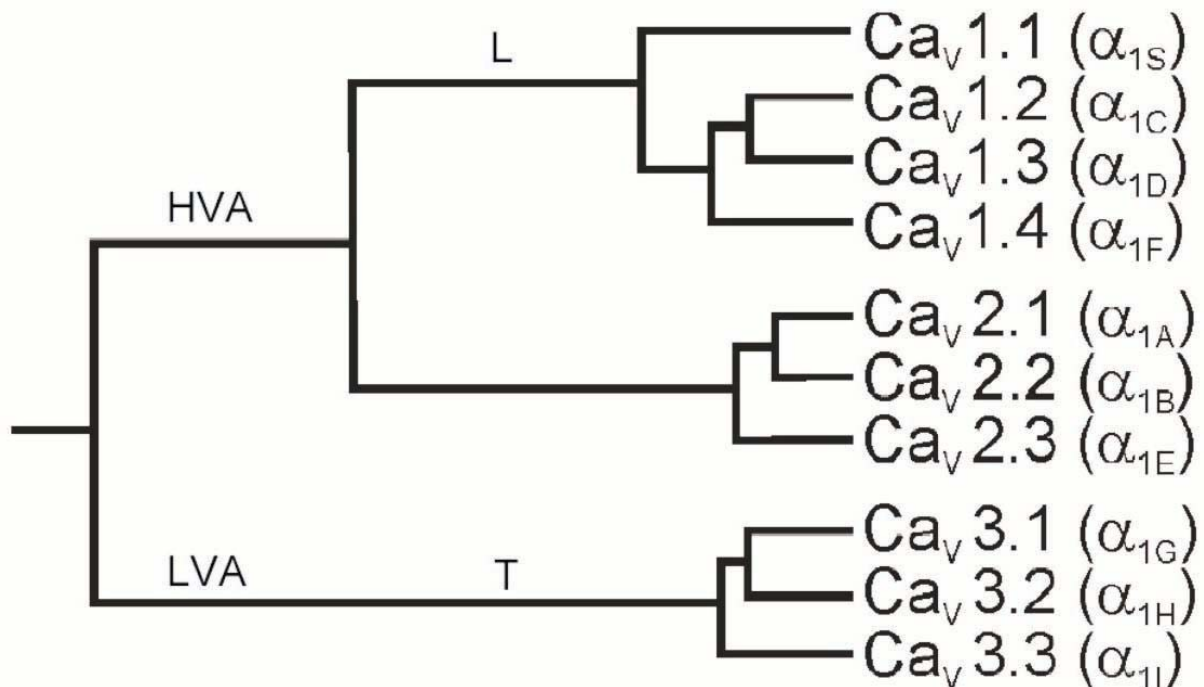


Figure 1-2 Phylogenetic representation of the primary sequences of the α_1 subunits of voltage-gated calcium channels. L-type calcium channels: $Ca_v1.1$ - $Ca_v1.4$, P/Q-type: $Ca_v2.1$, N-type: $Ca_v2.2$, R-type: $Ca_v2.3$, T-type: $Ca_v3.1$ - $Ca_v3.3$.

1.2 L-type calcium channels

LTCCs are one of the best characterized calcium channels today. They are distributed over a wide range of tissues and different isoforms are often expressed together in single cells or tissues (Table 1-1).

Table 1-1 Channel distribution and physiological function of LTCCs.

| name | splice variants | primary tissues | physiological function | Mutations and pathophysiology |
|---------------------|----------------------|---|---|--|
| Ca _v 1.1 | | skeletal muscle ¹ | excitation-contraction coupling, Ca ²⁺ homeostasis ¹ | Malignant hyperthermia ² |
| | Ca _v 1.2a | heart ¹ | action potential propagation ¹ | Timothy syndrome ³ ; |
| Ca _v 1.2 | Ca _v 1.2b | smooth muscle ¹ | excitation-contraction coupling ¹ | 1.2 deficient mice show multiple phenotypes ^{1,4,5} |
| | Ca _v 1.2c | neurons ¹ | synaptic plasticity ¹ | |
| Ca _v 1.3 | | brain, pancreas, kidney, heart ¹ | hormone release, regulation of transcription, synaptic integration ¹ | KO mice are deaf and show sinoatrial node dysfunction ⁶ |
| Ca _v 1.4 | | retina ^{1,7} | neurotransmitter release ^{1,8,9} | CSNB2 ^{1,8,9} |

References:

- ¹Catterall, W. A., Perez-Reyes, E., Snutch, T. P. & Striessnig, J. International Union of Pharmacology. XLVIII. Nomenclature and structure-function relationships of voltage-gated calcium channels. *Pharmacol Rev* **57**, 411-25 (2005)
- ²Striessnig, J. et al. L-type Ca²⁺ channels in Ca²⁺ channelopathies. *Biochem Biophys Res Commun* **322**, 1341-6 (2004)
- ³Liao, P., Yong, T. F., Liang, M. C., Yue, D. T. & Soong, T. W. Splicing for alternative structures of Cav1.2 Ca²⁺ channels in cardiac and smooth muscles. *Cardiovasc Res* **68**, 197-203 (2005)
- ⁴Seisenberger, C. et al. Functional embryonic cardiomyocytes after disruption of the L-type alpha1C (Cav1.2) calcium channel gene in the mouse. *J Biol Chem* **275**, 39 193-9 (2000)
- ⁵Schulla, V. et al. Impaired insulin secretion and glucose tolerance in beta cell-selective Ca(v)1.2 Ca²⁺ channel null mice. *Embo J* **22**, 3844-54 (2003)
- ⁶Platzer, J. et al. Congenital deafness and sinoatrial node dysfunction in mice lacking class D L-type Ca²⁺ channels. *Cell* **102**, 89-97 (2000)
- ⁷Firth, S. I., Morgan, I. G., Boelen, M. K. & Morgans, C. W. Localization of voltage-sensitive L-type calcium channels in the chicken retina. *Clin Experiment Ophthalmol* **29**, 183-7 (2001)
- ⁸Bech-Hansen, N. T. et al. Loss-of-function mutations in a calcium-channel alpha1-subunit gene in Xp11.23 cause incomplete X-linked congenital stationary night blindness. *Nat Genet* **19**, 264-7 (1998)
- ⁹Mansergh, F. et al. Mutation of the calcium channel gene Cacna1f disrupts calcium signaling, synaptic transmission and cellular organization in mouse retina. *Hum Mol Genet* **14**, 3035-46 (2005)

In summary, the criteria for their identification are the sensitivity to dihydropyridines, the relative slow activation kinetics, activation by strong depolarization, a large single channel conductance and the presence of calcium dependent inactivation (CDI) with little voltage dependent inactivation (VDI)⁵. Nevertheless, there are functional differences between LTCCs. Ca_v1.3 channels e.g., unlike Ca_v1.2 channels, have a low activation threshold, they only need weak depolarizations for activation⁶⁻¹⁰ and not all LTCCs show the same sensitivity to dihydropyridines (DHPs). Ca_v1.3 channels are significantly less sensitive to DHPs compared to Ca_v1.2 channels^{6,10}. The properties of Ca_v1.4 are not very well known at the moment.

1.3 Structure and regulation of the $\alpha 1$ subunit

The $\alpha 1$ subunit of the LTCC complex confers the basic pharmacological and electrophysiological properties of the calcium current. The subunit consists of four homologous domains (I-IV), each containing six transmembrane segments (S1-S6, Figure 1-3). The S4 segment acts as the voltage sensor of the channel and the pore loop located between the S5 and the S6 segment determines the ion conductance and selectivity¹.

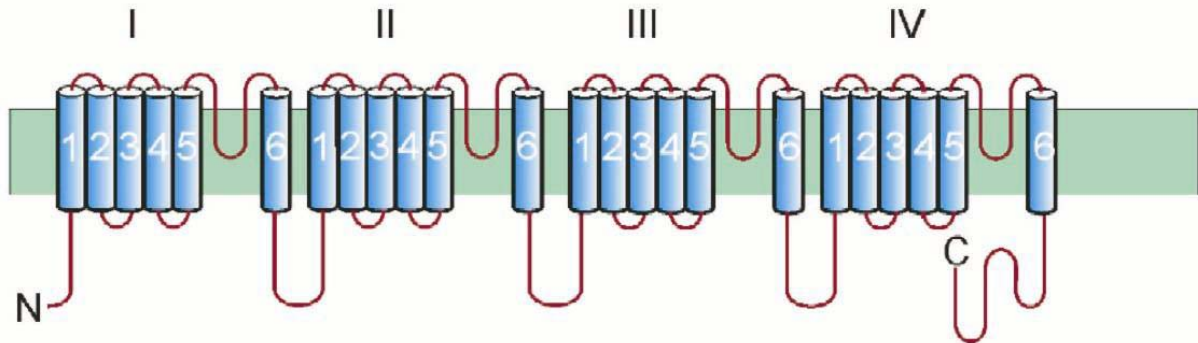


Figure 1-3 Schematic representation of an $\alpha 1$ L-type calcium channel subunit. It comprises four domains, each consisting of six transmembrane segments. The N- and the C-terminus are located at the cytosolic side of the membrane.

1.3.1 Pharmacological regulation of L-type calcium channels

Most of the known sites for channel regulation by toxins and drugs are also located in the $\alpha 1$ subunit. Phenylalkylamines block the pore of the channel from the intracellular side. Their binding site is formed by amino acids in the IIIS6 and IVS6 segment¹¹⁻¹³ (Figure 1-4). Unlike phenylalkylamines dihydropyridines (DHPs) do not block the channel pore, they rather allosterically shift the channel to the open or inactivated state. Thus, DHPs can be inhibitors as well as activators of LTCCs. Their receptor site is formed by amino acids in the IIIS5, the IIIS6 and the IVS6 segment. The amino acid residues important for the binding of phenylalkylamines and dihydropyridines are overlapping (Figure 1-4). The binding site for benzothiazepines also overlaps with the binding site for phenylalkylamines¹³.

| | IIIS5 | | IIIS6 | | | | IVS6 | | | | | |
|-----|----------|----------|-------------|-----------|----------|-------------|-----------|-----------|----------|-----------|----------------------|--------|
| | <i>d</i> | <i>d</i> | <i>pp</i> | <i>dd</i> | <i>d</i> | <i>dddd</i> | <i>pp</i> | <i>b</i> | <i>b</i> | <i>b</i> | | |
| | | | <i>dd</i> | | | | <i>dd</i> | <i>pp</i> | <i>p</i> | <i>pp</i> | | |
| 1.1 | IVLV | TLLC | FMFACIGVQLF | ---- | AIFFII | YII | IAFFMMNI | FV | GFVI | --- | FAYYFISFYMLCAFLIINL | LFVAVI |
| 1.2 | IVIV | TLLC | FMFACIGVQLF | ---- | SIFFII | YII | IAFFMMNI | FV | GFVI | --- | FAVFYFISFYMLCAFLIINL | LFVAVI |
| 1.3 | IMIV | TLLC | FMFACIGVQLF | ---- | SIFFII | YII | IAFFMMNI | FV | GFVI | --- | FAIVYFISFYMLCAFLIINL | LFVAVI |
| 1.4 | IMIV | TLLC | FMFACIGVQLF | ---- | SVFFIV | YII | IAFFMMNI | FV | GFVI | --- | FAIVYFISFFMLCAFLIINL | LFVAVI |

Figure 1-4 Alignment of amino acid residues of Ca_v1.1-Ca_v1.4 that participate in the formation of the dihydropyridine (*d*), phenylalkylamine (*p*) and benzothiazepine (*b*) binding sites. Important amino acid residues are highlighted red. Further benzothiazepine binding sites are supposed to be located in the IIIS6 segment but this remains to be confirmed on the single amino acid level¹³. Lower case letters indicate the contribution of the residue to the respective binding site.

1.3.2 Regulation by voltage and Ca²⁺ ions

The opening of ion channels and, hence, the flux of ions into or out of the cell is limited by a process designated as inactivation. In voltage-regulated ion channels inactivation is primarily conferred by depolarization (voltage dependent inactivation, VDI). Voltage-regulated calcium channels exhibit an additional inactivation mechanism, called calcium dependent inactivation (CDI). The term CDI describes the property of Ca²⁺ ions to limit its own influx by a feedback inhibition. In most cell types this autoinhibition is essential to prevent excessive and potentially toxic Ca²⁺ levels.

The mechanism of inactivation is not fully understood at the moment. The current view on LTCCs is mainly based on experiments with $Ca_v1.2$. In this channel VDI and CDI are highly interlinked with each other on a molecular level. One structural requirement for inactivation seems to be the cytoplasmatic linker between domain I and II. This linker is supposed to form a blocking particle (pore occluder, Figure 1-5, grey ball) that closes the pore when the channel inactivates¹⁴⁻¹⁶. Another structural determinant crucial for inactivation is the cytosolic proximal C-terminus comprising an EF-hand motif, an IQ motif and the Pre-IQ motif, which corresponds to the sequence stretch between the EF-hand and the IQ motif¹⁷. This proximal C-terminus is highly conserved among all HVA calcium channels¹⁷⁻²⁹. In the resting state the pore occluder (PO) is tonically inhibited by the EF-hand motif residing in the proximal C-terminus (Figure 1-5, left)³⁰. Maintained membrane depolarization results in a slow conformational change that breaks the tonic inhibition of the PO by the EF-hand. Thus, the PO closes the pore of the channel (VDI).

The sequences conferring CDI are the EF-hand motif, the Pre-IQ and the IQ motif (Figure 1-5)¹⁷⁻²⁹. In the absence of Ca^{2+} ions, Ca^{2+} -free calmodulin (apocalmodulin) is prebound to the proximal C-terminus, more exactly to the area of the IQ and the Pre-IQ motif (Figure 1-5, left)^{21,25}. Apocalmodulin is a calcium sensor comprising four EF-hands grouped in the N-lobe with low affinity and the C-lobe with high affinity for Ca^{2+} ions³¹. When Ca^{2+} influx starts, the Ca^{2+} concentration at the intracellular side of the pore increases and, for LTCCs, Ca^{2+} binds to the C-lobe of calmodulin¹⁸. Subsequently Ca^{2+} -calmodulin translocates to its effector site near the apocalmodulin binding region and thereby induces a fast conformational change of the proximal C-terminus. Thus the EF-hand accelerates the movement of the PO actively and the channel inactivates much faster^{23,30}. As Figure 1-5 shows, the sequences conferring CDI in $Ca_v1.2$ are highly conserved in $Ca_v1.4$.

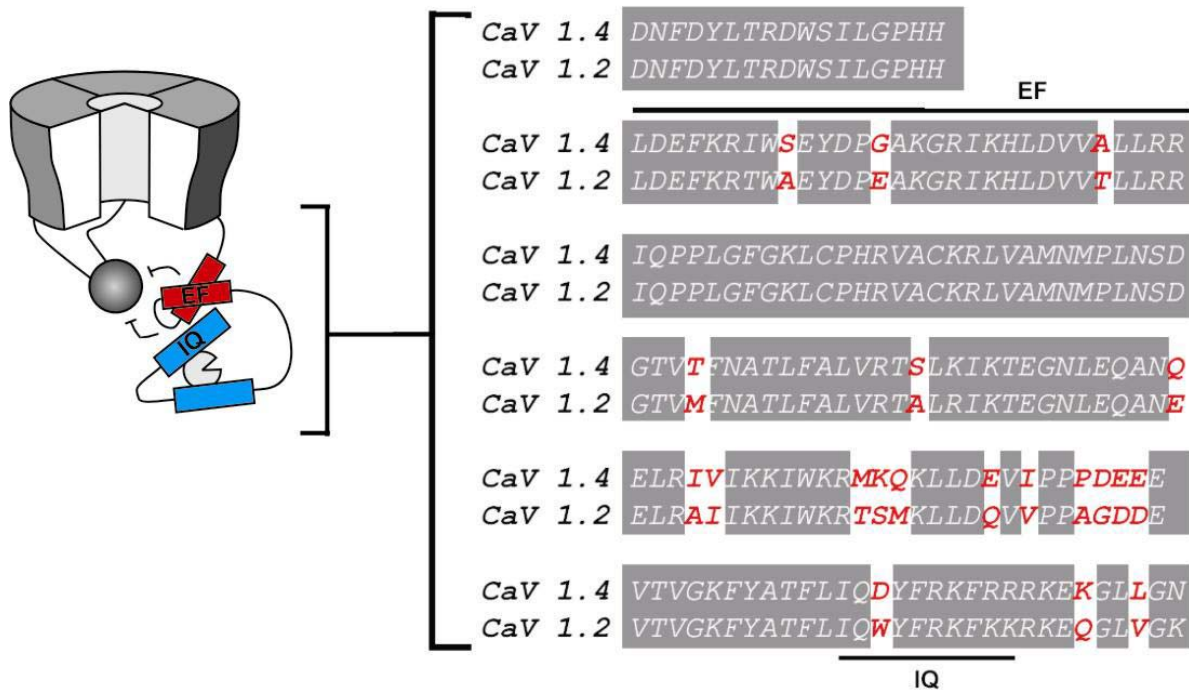


Figure 1-5 Left: So far established structural determinants of inactivation in Cav1.2. The pore occluder is shown as grey ball. The bars indicate the tonic inhibition by the EF-hand. Calmodulin (light grey) is prebound to the C-terminus. The distal part of the C-terminus is not shown.

Right: Alignment of the C-termini of Ca_v1.4 α 1 and Ca_v1.2 β 1 from the end of the IVS6 segment to the end of the IQ motif. The sequences conferring CDI (EF hand, Pre-IQ and IQ motif) are highly conserved. Bars on top of the alignment indicate the borders of EF-hand motif and IQ-motif. The sequence stretch between this two motifs is the Pre-IQ area. Differences in the primary sequence are indicated as red letters.

1.4 Physiological impact of Ca_v1.4 α 1

Photoreceptor cells contain specialized synaptic terminals, so-called ribbon synapses, that confer the release of glutamate. In the dark, when the membrane potential is rather depolarized (-40mV), glutamate is tonically released at these synapses. Light induces a hyperpolarization and, hence, switches off neurotransmission. Voltage-gated calcium channels are known to play a key role in synaptic transmission. They couple depolarization of the membrane potential with an influx of Ca²⁺ ions into the cell which is the trigger for exocytosis. At the ribbon synapses several types of LTCCs have been detected, namely Ca_v1.2, Ca_v1.3 and Ca_v1.4^{32,33}. As the only one of the three channels Ca_v1.4 seems to be specifically expressed in the retina^{34,35}. L-type calcium currents measured from retinal photoreceptor or bipolar cell differ from other L-type calcium currents in lacking CDI³⁶⁻⁴¹ (Figure 1-6).

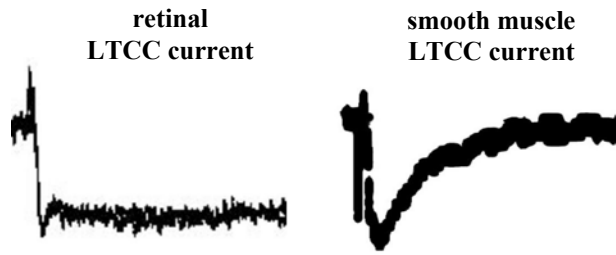


Figure 1-6 Calcium currents measured from a rod bipolar cell (left, Berntson et al. (2003) *J Neurosci Res* **19**, 260) and a tracheal myocyte (right, Fleischmann et al. (1994) *Proc. Natl. Acad. Sci. USA* **91**, 11914-11918). Retinal LTCC currents show no inactivation in the presence of Ca^{2+} ions.

This property is required in the dark to ensure a permanent glutamate release at depolarized voltages. $\text{Ca}_v1.2$ and $\text{Ca}_v1.3$ channels display CDI, thus, it is likely that the lack of CDI in native L-type calcium currents from retinal cells is due to $\text{Ca}_v1.4$ or to other factors that modify channel function. The importance of $\text{Ca}_v1.4$ is corroborated by genetic studies. While mice lacking $\text{Ca}_v1.2$ or $\text{Ca}_v1.3$ show no visual impairment, the loss of $\text{Ca}_v1.4$ leads to severe disorder, called incomplete X-linked congenital stationary night blindness type 2 (CSNB2)⁴². CSNB2 is characterized by symptoms like myopia, nystagmus, night blindness and low visual acuity. This phenotype is consistent with a defect in neurotransmission in the retina^{32,34,35,43,44}. Also in humans mutations in the gene coding for $\text{Ca}_v1.4\alpha1$ are known that lead to CSNB2^{43,44}. The molecular mechanism by which this loss of function mutations of $\text{Ca}_v1.4$ lead to CSNB2 is not fully understood at the moment. However, these data indicate that $\text{Ca}_v1.4$ plays a key role in vision.

The tissue distribution and the physiological properties of the auxiliary LTCC subunits are only moderately known. Only the $\beta2$ subunit, which increases expression levels and modulates the gating properties of the channel complex, is exactly known to be localized in the retina. The expression of this subunit is required for normal retinal synaptic transmission just as well as the $\text{Ca}_v1.4\alpha1$ subunit⁴⁵.

1.5 Purpose of the study

As stated above it was unclear whether the properties of the retinal L-type calcium currents are conferred by $Ca_v1.4$ or are rather due to other regulatory mechanisms. To clarify this question, the $Ca_v1.4\alpha1$ L-type calcium channel subunit shall be cloned from mouse retina and heterologously expressed in HEK cells. Afterwards, the basic biophysical and pharmacological properties have to be determined in electrophysiological experiments in order to be compared with native LTCC currents from retina.

Based on the previous analysis the mechanism of CDI is addressed in the second part of this study. As mentioned, there was preliminary evidence that $Ca_v1.4$ channels may lack CDI despite its high homology to other LTCCs. The purpose of this study is to identify structural determinants that prevent CDI in $Ca_v1.4$ in order to explain this phenomenon.

2 MATERIALS AND METHODS

All chemicals used meet the standard “pro analysi” (p.a.). For generation of all solutions desalted high purity water (Easypure UV/UF, Barnstead) was used. Solutions for highly sensitive applications (e.g. PCR, cell culture) or solutions designed for long term use were autoclaved.

2.1 Calcium channel constructs

All constructs mentioned in the text were tested for integrity by enzymatic restriction analyses and DNA sequencing. Sequencing was performed by MWG-Biotech. All restriction endonucleases used are products of New England Biolabs, Inc. All primers used are products of MWG-Biotech (Table 6-1).

2.1.1 Constructs for electrophysiology

For expression of murine $Ca_v1.4\alpha1$ LTCC subunit (GenBank accession number AJ579852) in eukaryotic cells the bicistronic pIRES2-EGFP expression vector (Clontech) was used⁴⁶. It contains the internal ribosome entry site (IRES) of the encephalomyocarditis virus between the multiple cloning site (MCS) and the enhanced green fluorescent protein (EGFP) coding region. As a result, both, $Ca_v1.4\alpha1$ and EGFP are expressed as separate proteins. Such transfected cells could easily be identified by fluorescence.

The pcDNA3 expression vector (Invitrogen) was used for expression of the $Ca_v1.2\beta\alpha1$ subunit from rabbit lung⁴⁷ in eukaryotic cells and for expression of a negativ dominant calmodulin mutant (CaM_{1234})⁴⁸, the $\beta2a$ ⁴⁹, the $\beta3$ ⁴⁹ and the $\alpha2\delta1$ subunit⁵⁰. $Ca_v1.2\beta\alpha1$, $\beta2a$, $\beta3$ and $\alpha2\delta1$ expression vectors were a gift of N. Klugbauer.

2.1.1.1 Construction of $Ca_v1.4\alpha1$ mutants

Truncated $Ca_v1.4$ channels (G1458Stop, R1610Stop, Y1668Stop, R1796Stop, C1884Stop, Q1930Stop, Q1953Stop) were constructed by ligating BamH I/Xho I cut DNA fragments generated via PCR and corresponding to the required C-terminal part of $Ca_v1.4\alpha1$ and a EcoR I/BamH I cut fragment corresponding to the proximal 3945bp of the plasmid encoding for wild type $Ca_v1.4\alpha1$ into the EcoR I/Sal I cut pIRES2-EGFP expression vector. The BamH I/Xho I cut fragments carried the required Stop codon and a Xho I restriction site immediately after the stop codon introduced by 3`-primers.

The Ca_v1.4ΔC channel was cloned by deleting amino acids R1610-C1884 of Ca_v1.4α1 using overlap PCR. Again, a Xho I restriction site was introduced by a 3'-primer and the PCR product was cut BamH I/Xho I. Ligation was performed as mentioned above.

For construction of the Ca_v1.4ΔEF channel amino acids P1459-I1491 were deleted in the same way.

The nucleotide sequence corresponding to the ICDI peptide (inhibitor of calcium dependent inactivation, amino acids L1885-L1984 of Ca_v1.4α1) was amplified by PCR. A BamH I restriction site, an optimized sequence for initiation of translation (Kozak sequence, GCC GCC ACC)⁵¹ and a start codon were introduced by the 5'-primer and a Xho I restriction site was introduced by the 3'-primer immediately after the stop codon. The BamH I/Xho I cut PCR product was ligated into the BamH I/Xho I cut pcDNA3 expression vector.

2.1.1.2 Construction of Ca_v1.2βα1 / Ca_v1.4α1 chimeric channels

In chimera 1.2-CT1.4 amino acids D1502-L2166 of Ca_v1.2βα1 were replaced by D1445-L1984 of Ca_v1.4α1 by several overlapping PCR steps. The PCR fragment was cut EcoR V/Apa I and ligated into the Hind III/Apa I cut pcDNA3 expression vector together with proximal, Hind III/EcoR V cut part of Cav1.2βα1.

In 1.2-ICDI1.4 G2018-L2166 of Ca_v1.2βα1 were replaced by L1885-L1984 of Ca_v1.4α1, in chimera 1.2ΔC-ICDI1.4 K1667-L2166 of Ca_v1.2βα1 were replaced by L1885-L1984 of Ca_v1.4α1, in 1.2-C+ICDI1.4 K1667-L2166 of Ca_v1.2βα1 were replaced by R1610-L1984 of Ca_v1.4α1 and in 1.2-A+ICDI1.4 K1667-L2166 of Ca_v1.2βα1 were replaced by R1610-L1984 of Ca_v1.4α1 with a deletion of I1742-C1884. All exchanges again were done via overlap PCR. The PCR fragments were cut BstE II/Xho I and ligated into the BstE II/Xho I cut Ca_v1.2βα1 expression vector.

In chimera 1.2-A1.4 amino acids K1667-L2166 of Ca_v1.2βα1 were replaced by amino acids R1610-S1741 via PCR. A stop codon and a BamH I restriction site immediately after the stop codon were introduced by the 3' primer. Following the BstE II/BamH I cut PCR fragment was ligated into the BstE II/BamH I cut Ca_v1.2βα1 expression vector.

2.1.2 Constructs for GST pull-down

For generation of glutathione-S-transferase (GST) fusion proteins the DNA fragments coding for the required peptides were amplified by PCR and cloned into the pET41a(+) expression

vector (Novagen), in frame with a upstream coding region for GST. This vector is designed for expression of GST fusion proteins in bacterial systems.

The nucleotide sequences corresponding to the C-terminal fragments of Ca_v1.4α1 or Ca_v1.2βα1, CT1.4 (amino acids D1445-L1984 of Ca_v1.4α1), CT1.4-1610Stop (amino acids D1445-G1609 of Ca_v1.4α1), CT1.4 1610-1984(amino acids R1610-L1984 of Ca_v1.4α1), CT1.2 (amino acids D1502-L2166 of Ca_v1.2βα1), CT1.2-1667Stop (amino acids D1502-G1666 of Ca_v1.2βα1) and CT1.2 1667-2166 (amino acids K1667-L2166 of Ca_v1.2βα1), were amplified via PCR, introducing a BamH I restriction site by the 5'-primer, an appropriate stop codon if required and a Xho I restriction site immediately after the stop codon by the 3'-primer. These BamH I/Xho I cut PCR fragments were ligated into the BamH I/Xho I cut pET41a(+) vector.

Cloning of peptide A (amino acids R1610-S1741 of Ca_v1.4α1) was performed in the same way, but the C-terminal restriction site was a BamH I and not a Xho I site. It was digested with BamH I and ligated into the BamH I cut pET41a(+) vector.

For ΔEF (amino acids D1445-G1609 of Ca_v1.4α1 with amino acids P1459-I1491 deleted) PCR was performed with the cDNA encoding for Ca_v1.4ΔEF (2.1.1) as a template. The same primers as for CT1.4-1610Stop were used and the BamH I/Xho I cut PCR fragment was ligated into a BamH I/Xho I cut pET41a(+) vector.

Generation of 6xHis/Flag tagged ICDI was performed as follows:

the DNA fragment encoding for the ICDI peptide (see 2.1.1) was amplified by PCR. A BamH I restriction site and a N-terminal Flag tag (amino acid sequence: D-Y-K-D-D-D-D-K) were introduced by the 5'-primer and a Xho I restriction site immediately after the stop codon was introduced by the 3'-primer. This BamH I/Xho I cut PCR fragment was ligated into the BamH I/Sal I cut pQE-30 vector (Quiagen) in frame with the upstream 6xHis tag. The pQE-30 expression vector is also designed for expression of peptides and proteins in bacterial systems.

2.1.3 Constructs for coimmunoprecipitation

For generation of the myc tagged C-terminal fragments CT1.4-1610Stop (amino acids see 2.1.2) and ΔEF (amino acids see 2.1.2), the encoding cDNA fragments were amplified by PCR. A BamH I restriction site, a Kozak sequence (see 2.1.1), a start codon and a N-terminal myc tag (amino acid sequence: E-Q-K-L-I-S-E-E-D-L) were introduced by the 5'-primer and an appropriate stop codon and a Xho I restriction site immediately after the stop codon by the 3'-primer. Generation of peptide A (amino acids see 2.2) and peptide C (amino acids R1610-C1884 of Ca_v1.4α1) was performed the same way, but the N-terminal restriction site

introduced was EcoR I. After digestion with the appropriate restriction enzymes the PCR fragments were cloned into the BamH I/Xho I and EcoR I/Xho I cut pcDNA3 vector, respectively.

The triple flag tagged ICDI peptide was constructed in the same manner using a 5`-primer containing a BamH I restriction site and the triple flag tag (amino acid sequence: D-Y-K-D-H-D-G-D-Y-K-D-H-D-I-D-Y-K-D-D-D-D-K) instead of the myc tag .

2.2 Amplification and purification of DNA

2.2.1 Transformation of competent *E. coli*

An aliquot of 100µl of competent Escherichia coli (*E. coli*; BL21(DE3) competent cells (Novagen) or XL1-blue competent cells (Stratagene)) was thawed on ice. 15µl of ligated DNA was added to the cells, mixed gently and kept on ice for further 30min. Afterwards the cells were exposed to a heat shock by placing the tube into a water bath at 42°C for 45sec and then left on ice for two minutes. 900µl autoclaved Luria-Bertani medium containing glucose (LB+ medium) was added and the tube was placed on a shaking incubator for 1h at 37°C and 225rpm. After centrifugation at 3000rpm for 5min the pellet was resuspended in 100µl LB+ medium and plated on LB+ agar plates containing the appropriate antibiotic (Ampicillin 50µg/ml, Roth; Kanamycin 30µg/ml, Roth). The agar plates were incubated for 16-20h at 37°C.

LB+ medium

| | |
|----------------------|-----------|
| Peptone (Roth) | 10g |
| Yeast extract (Roth) | 5g |
| NaCl (Roth) | 5g |
| Glucose (Roth) | 1g |
| H ₂ O | ad 1000ml |
| pH 7.2-7.5 | |

LB+ agar

| | |
|-------------|-----------|
| Agar (Roth) | 15g |
| LB+ medium | ad 1000ml |

2.2.2 Mini-Prep DNA isolation from *E. coli*

To check if the isolated single colonies contained the correct plasmid, Mini-Prep DNA isolation was performed. Single colonies from the agar plate were cultured in 7ml LB+ medium containing Ampicillin 100µg/ml and Kanamycin 30µg/ml, respectively, and placed on a shaking incubator for 12-16h at 37°C and 225rpm. After harvesting the bacterial cells by centrifugation (2000g, 10min) alkaline lysis⁵² was performed for isolation of the plasmid DNA.

After isolation enzymatic restriction analysis was performed.

2.2.3 Maxi-Prep DNA isolation from *E. coli*

To recover larger amounts of high-purity DNA the PureYield™ Plasmid Midiprep System (Promega) was used. It is based on the method of alkaline lysis⁵² in combination with purification by a silica membrane column.

Before, bacteria containing the correct plasmid were cultured in 200ml LB+ medium containing the appropriate antibiotic for 12-16h under the conditions mentioned above (2.2.2).

Cells were centrifuged at 5000g for 10min after incubation and DNA was isolated.

Enzymatic restriction analysis and DNA sequencing (MWG-Biotech) were performed to confirm integrity of the plasmids.

2.3 Cell culture

All procedures described were carried out under sterile conditions under a laminar air flow.

2.3.1 Culture of HEK 293 cells

The HEK 293 cell line is established from human primary embryonal kidney transformed by adenovirus type 5⁵³. The cells were cultured in Dulbecco's modified eagle medium (DMEM, Gibco) containing 1000mg glucose supported with 10% fetal bovine serum (FBS, Biochrom), 100U/ml Penicillin G (Biochrom) and 100µg/ml Streptomycin (Biochrom) in a 75cm² culture flask (Sarstedt) at 10% CO₂ and 37°C. Cells were splitted every 2-3 days when they had reached about 80% confluence. When splitted, cells were washed with phosphate buffered saline (PBS) and disaggregated by using a solution of 0.05% trypsin containing 0.02% ethylenediamine tetraacetic acid (EDTA). After inactivation of trypsin by the addition of DMEM cells were resuspended and again disaggregated by mechanic influence. 10% of the cells were seeded out in a new 75cm² culture flask.

Every 3 weeks a new stock of cells was thawed from -196°C.

PBS, pH 7.4

| | |
|---|-----------|
| NaCl (Roth) | 40.0g |
| KCl (Roth) | 1.0g |
| Na ₂ HPO ₄ *12H ₂ O (Roth) | 14.5g |
| KH ₂ PO ₄ (Roth) | 1.2g |
| H ₂ O | ad 5000ml |

0.05% trypsin/0.02% EDTA

| | |
|---|----------|
| Stock solution (0.5% trypsin/0.2% EDTA, Biochrom) | 10ml |
| PBS | ad 100ml |

2.3.2 Transient transfection of HEK 293 cells for coimmunoprecipitation

Cells were grown in a 10cm culture dish containing 10ml medium. When they had reached about 80% confluence, cells were transfected using the calcium phosphate method⁵⁴ with a modified buffer⁵⁵.

2.3.3 Transient transfection of HEK 293 cells for electrophysiology

About 3×10^5 cells were seeded into each well of a 6-well culture plate containing 2ml of culture medium. 4-6h after seeding the cells they were transfected using Fugene 6 Transfection Reagent (Roche). The ratio of DNA (μg) and Fugene 6 (μl) was 1:3. The total reaction volume for complexation was ten times the volume of Fugene 6. Besides transfection was done following the manufacturer's instructions.

2.4 Analysis of proteins

2.4.1 *GST pull-down assay*

For all steps described below protease inhibitors (PI; Complete, EDTA free; Roche) were added to the solutions according to the manufacturer's instructions. All steps were performed at 4°C.

2.4.1.1 *Purification of GST fusion proteins expressed in E. coli*

GST fusion proteins were expressed in the protease deficient BL21 (DE3) strain of *E. coli*. (Novagen). Transformation was performed as described above (2.2.1), except that the bacteria were diluted in 50ml LB- medium (LB+ medium without glucose) containing the appropriate antibiotic after incubation at 37°C for 1h on a shaking incubator. The bacteria were grown over night at the same conditions. Next morning they were diluted in 500ml LB- medium containing antibiotics. Bacteria were grown until they reached an OD₆₀₀ of about 0.6-0.8. Then expression of fusion proteins was induced by adding isopropyl-β-D-thiogalactopyranoside (IPTG, Roth) to a final concentration of 1mM. The culture was incubated again at 37°C on a shaking incubator. After 4h bacteria were pelleted by centrifugation (10min, 4°C, 5000g), resuspended in 20ml ST buffer (50mM a,a,a-Tris-(hydroxymethyl)-methylamin (Tris), pH 8, VWR; 150mM NaCl, VWR) supplemented with 100μg/ml lysozyme (Roth). After incubation on ice for 15min dithiothreitol (DTT; Sigma) was added to a final concentration of 5 mM and the suspension was incubated on ice for further 10 min. N-lauroylsarcosine (Sigma) was added to a final concentration of 1%. After 30 min incubation on ice the mixture was sonicated on ice (Bandelin Sonopulse HD2200 with a MS-73 tip) by 6 pulses of 40s duration at 50% power separated by 30s cooling periods. Triton X-100 (Sigma) was added to a final concentration of 1.5%, and after 30 min on ice the lysate was clarified by centrifugation at 12,000 × g for 20 min at 4°C. The pellet was discarded and the supernatant was split in 1ml aliquots and frozen at -80°C.

2.4.1.2 *Expression of 6xHis/Flag tagged ICDI peptide in E. coli*

For expression of the 6xHis/Flag tagged ICDI peptide XL1-blue competent cells (Stratagene) were used. The rest of the procedure was done as described in 2.4.1.1.

2.4.1.3 *Measurement of GST fusion protein concentration*

An aliquot of the lysate containing the required GST fusion protein was thawed on ice and the concentration of the fusion protein was estimated enzymatically by measuring the activity of GST using the GST TagTM Assay Kit (Novagen).

2.4.1.4 *Measurement of overall protein concentration*

The overall protein concentration in lysates was measured by Bradford assay⁵⁶.

2.4.1.5 *Interaction with calmodulin*

Glutathione sepharose beads (Glutathion Sepharose 4B, Amersham Biosciences) were washed three times in 10 bed volumes ST buffer. After each wash the beads were centrifuged (2min, 500g, 4°C) and after the last wash they were resuspended in 1 bed volume ST buffer. 50µl of the suspension were added to a portion of crude protein extract corresponding to 300pmol of the required GST fusion protein. The resulting mixture was rotated over night at 4°C. Next morning the beads were centrifuged (2min, 500g, 4°C), kept on ice for 1min and the supernatant was discarded. Afterwards the beads were washed as mentioned above in 20 bed volumes ST buffer and resuspended in 1ml ST buffer in the presence of 1mM CaCl₂ (Merck) respectively 5mM EGTA (Sigma). 1µg calmodulin (bovine brain, Calbiochem) was added. The mixture was rotated for 2h at 4°C. After centrifugation (2min, 500g, 4°C) the beads were washed three times as mentioned in 20 bed volumes of the same buffer they were incubated containing 0.05% Tween-20 (Roth). After washing, the beads were resuspended in 25µl ST buffer.

2.4.1.6 *Interaction with ICDI*

Glutathion sepharose beads were prepared as above. 300 pmol of the required GST fusion protein were mixed with 50µl beads suspension and a portion of crude protein extract containing the 6xHis/Flag tagged ICDI peptide matching 250µg overall protein. ST buffer was added to a final volume of 1ml. This mixture was rotated overnight at 4°C. The next day beads were centrifuged (2min, 500g, 4°C), kept on ice for 1min and the supernatant was discarded. Afterwards the beads were washed four times in 20 bed volumes ST buffer containing 0.05% Tween-20. After washing beads were resuspended in 25µl ST buffer.

2.4.2 Coimmunoprecipitation

For all steps described below protease inhibitors (PI; Complete, EDTA free; Roche) were added to the solutions, according to the manufacturer's instructions. All steps were performed at 4°C.

2.4.2.1 Purification of proteins expressed in HEK 293 cells

Transfection of HEK 293 cells was performed as described in 2.3.2. 16-20h after transfection the medium was exchanged and 3d after transfection the cells were washed with 10ml PBS and lysed with 500µl lysis buffer (50mM TRIS-HCl, pH 7.4, Roth; 150mM NaCl, VWR; 1mM EDTA, Roth and 1% Triton X-100, Sigma). The culture dishes were placed on an orbital shaker for 30min at 4°C and 100rpm. The lysed cells then were scraped off the dish, transferred into a reaction tube and centrifuged (15min, 12000g, 4°C). The pellet was discarded and the supernatant was frozen at -80°C for further use.

2.4.2.2 Quantification of proteins

Overall protein concentration was measured as described in 2.4.1.4

2.4.2.3 Coimmunoprecipitation of proteins

Protein A sepharose beads (Amersham biosciences) were washed three times in 10 bed volumes AM0 buffer (20 mM TRIS-HCl pH7.9, Roth; 5 mM MgCl₂, Merck; 0.5 mM DTT, Sigma; 20% glycerol, Roth) and resuspended in 1 bed volume AM0 buffer. After each wash the beads were centrifuged (2min, 500g, 4°C). Protein extracts containing the required myc tagged C-terminal fragment of Ca_v1.4α1 and the triple flag tagged ICDI peptide were mixed (500µg overall protein, each) and 40µl of beads suspension and AM0 buffer were added to a final volume of 500µl. For immunoprecipitation 5µg of anti-myc antibody (mouse monoclonal IgG, Cell signalling) or 5µg of anti-ras antibody (control antibody, mouse monoclonal IgG, Santa Cruz Biotechnology) were used. This mixture was rotated over night at 4°C. The next day, beads were pelleted by centrifugation (2min, 500g, 4°C) and washed four times as described with AM100 buffer (AM0 buffer supplemented with 100mM KCl, Roth). After centrifugation the beads were resuspended in 25µl AM0 buffer.

2.4.3 Western blot analysis

2.4.3.1 SDS-polyacrylamid gel electrophoresis (SDS-PAGE)

Proteins were separated by SDS-PAGE using the method described by Laemmli⁵⁷. After adding 6xLaemmli sample buffer to the samples, they were boiled 5min at 98°C. For electrophoresis the Mini-PROTEAN 3 electrophoresis system (Biorad) was used. Thickness of the gels was 1.5mm. The concentration of acrylamid/bisacrylamid solution (Rotiphorese Gel 30, 37.5:1, Roth) in the resolving gel depended on the protein to be analyzed. Electrophoresis was done at 100V. As protein standards the Precision Plus Protein™ Kaleidoscope™ Standards (Biorad) were used.

The following solutions were used:

4xTris-HCl/SDS pH6.8

(0.5M Tris, 0.4% SDS)

| | |
|--------------------------------|----------|
| Tris (VWR) | 6.0g |
| SDS ultra pure (Roth) | 0.4g |
| H ₂ O | ad 100ml |
| pH 6.8 adjustet with HCl (VWR) | |

6xLaemmli sample buffer

| | |
|-------------------------|---------|
| 4xTris-HCl/SDS pH6.8 | 7ml |
| Glycerol (Roth) | 3ml |
| SDS ultra pure (Roth) | 1.0g |
| Bromphenol blue (Merck) | 0.004% |
| DTT (Sigma) | 0.9g |
| H ₂ O | ad 10ml |

4xTris-HCl/SDS pH8.8

(1.5M Tris, 0.4% SDS)

| | |
|--------------------------|----------|
| Tris (VWR) | 18.2g |
| SDS ultra pure (Roth) | 0.4g |
| H ₂ O | ad 100ml |
| pH 8.8 adjustet with HCl | |

Stacking gel

| | |
|---|--------|
| Rotiphorese Gel 30 (Roth) | 0.65ml |
| 4xTris-HCl/SDS pH6.8 | 1.25ml |
| H ₂ O | 3.05ml |
| TEMED (Sigma) | 5µl |
| Ammonium peroxodisulphate (Roth, 20% solution in H ₂ O) | 25µl |

10xElectrophoresis buffer

| | |
|-----------------------|-----------|
| Tris (VWR) | 30.2g |
| Glycine (Roth) | 144.0g |
| SDS ultra pure (Roth) | 10.0g |
| H ₂ O | ad 1000ml |

Resolving gel (7%-15%)

| | |
|---|-------------|
| Rotiphorese Gel 30 (Roth) | 3.50-7.50ml |
| 4xTris-HCl/SDS pH8.8 | 3.75ml |
| H ₂ O | 7.75-3.75ml |
| TEMED (Sigma) | 10µl |
| Ammonium peroxodisulphate (20% solution in H ₂ O) | 30µl |

2.4.3.2 Immunological detection of proteins

For immunological detection the proteins separated by SDS-PAGE were electroblotted to a Immun-Blot PVDF (polyvinylidene difluoride) Membrane (Biorad) with a pore size of 0.2µm or 0.45µm depending on the molecular weight of the respective protein.

For blotting of calmodulin CaM transfer buffer was used. The resolving gel was equilibrated in CaM transfer buffer for 10min before blotting. Calmodulin was transferred at 100mA for 35min. After blotting, the PVDF membrane was dried for 1h at 37°C and then it was wet with methanol (Roth) and blocked with tris buffered saline (TBS) containing 3% milk powder (Fluka) for 15min at room temperature. Incubation with anti-calmodulin antibody (mouse monoclonal IgG, Upstate) as primary antibody was done over night at 4°C. The antibody concentration was 1µg/ml and it was diluted in TBS containing 3% milk powder and 0.05% sodium azide (Roth). After washing the membrane three times for 5min in TBS it was incubated with anti-mouse IgG antibody conjugated with horseradish peroxidase (Amersham biosciences) for 1h at room temperature. The secondary antibody was diluted 1:5000 in TBS containing 3% milk powder. The membrane was washed as described above and the protein was detected by enhanced chemiluminescence using the ECLTM Western Blotting Analysis System (Amersham Biosciences). The Blot was exposed to a light sensitive film (Hyperfilm ECLTM, Amersham Biosciences).

For blotting of ICDI peptide ICDI transfer buffer was used and the peptides were transferred at 200mA for 35min. An anti-flag antibody (mouse monoclonal IgG, Sigma) at a concentration of 2.5µg/ml was used as primary antibody. Incubation was performed at room temperature for 1h. The rest of the procedure was done as mentioned above.

Blotting of GST and myc fusion proteins was performed with normal transfer buffer at 300mA for 1h. An anti-GST antibody (mouse monoclonal IgG, Novagen) and an anti-myc antibody (mouse monoclonal IgG, Cell signaling), respectively, were used as primary antibodies. Immunological detection was performed according to the manufacturer's instructions.

Solutions used:

CaM transfer buffer

(CaCl₂ 2mM, methanol 35%)

| | |
|---------------------------|-----------|
| Tris (VWR) | 3.02g |
| Glycine (Roth) | 14.4g |
| CaCl ₂ (Merck) | 0.29g |
| Methanol (Roth) | 350ml |
| H ₂ O | ad 1000ml |

transfer buffer

(methanol 20%)

| | |
|---------------------------|-----------|
| 10xElectrophoresis buffer | 100ml |
| (see 2.4.3.1) | |
| Methanol (Roth) | 200ml |
| H ₂ O | ad 1000ml |

ICDI transfer buffer

(methanol 35%)

| | |
|---------------------------|-----------|
| 10xElectrophoresis buffer | 100ml |
| (see 2.4.3.1) | |
| Methanol (Roth) | 350ml |
| H ₂ O | ad 1000ml |

10xTBS pH8

| | |
|------------------------------|-----------|
| Tris (VWR) | 12.1g |
| NaCl (Merck) | 80.2g |
| H ₂ O | ad 1000ml |
| pH 8.0 was adjusted with HCl | |

2.5 Electrophysiology

2.5.1 Performance

Unless otherwise noted, HEK293 cells were transiently transfected with expression vectors encoding for $Ca_v1.4\alpha1$ or $Ca_v1.2b\alpha1$, together with equimolar amounts of vectors encoding for $\beta2a$ or $\beta3$ and $\alpha2\delta1$ as described (2.3.3).

Currents were measured at room temperature 2-4d after transfection using the whole-cell patch-clamp technique. Data were acquired using an Axopatch 200B amplifier (Axon Instruments) and Clampex 8.2 software (Axon Instruments). Data were analyzed using Clampfit 8.2 (Axon Instruments) and Origin 6.1 (Originlab Corporation) software.

Patch pipettes were pulled from borosilicate glass capillaries with an outer diameter of 1.5mm and an inner diameter of 1.17mm (Harvard Apparatus). The pipette resistance varied from 1.5 to 2.5M Ω . Cell sizes ranged between 15 and 60pF and the access resistances were between 3.0 and 7.0M Ω and were compensated up to 70%. I_{Ca} and I_{Ba} were measured from the same cell.

Following solutions were used for current measurements:

Pipette solution

| | |
|------------------------------------|---------|
| CsCl (Sigma) | 112.0mM |
| MgCl ₂ (Merck) | 3.0mM |
| MgATP (Sigma) | 3.0mM |
| EGTA (Sigma) | 10.0mM |
| HEPES (Sigma) | 5.0mM |
| pH7.4 adjusted with CsOH (Aldrich) | |

Bath solution

(30mM BaCl₂)

| | |
|---------------------------------------|--------|
| NaCl (Merck) | 82.0mM |
| BaCl ₂ (Sigma) | 30.0mM |
| CsCl (Sigma) | 5.4mM |
| MgCl ₂ (Merck) | 1.0mM |
| TEA (Sigma) | 20.0mM |
| HEPES (Sigma) | 5.0mM |
| Glucose (Merck) | 10.0mM |
| pH 7.4 was adjusted with NaOH (Merck) | |

For experiments with 10mM BaCl₂ or 10mM CaCl₂ in the bath solution the NaCl concentration was increased to 102mM. Bath solutions were exchanged and drugs were applied by a local solution exchanger and reached the cell membrane within less than 100ms. Drugs applied were: racemic verapamil hydrochloride (Sigma), D-(+)-cis-diltiazem hydrochloride (Sigma), L-(-)-cis-diltiazem hydrochloride (Biomol Research Laboratories Inc.), racemic isradipine (Novartis) and S-(-)-Bay K8644 (Sigma). Stock solutions of the drugs were prepared in H₂O or ethanol (isradipine). For experiments stock solutions were diluted in the required bath solution.

2.5.2 *Protocols*

I-V curves were measured by applying 150 or 350ms voltage pulses to potentials between -80 and 70mV in 10mV increments from a holding potential of -80mV at 0.2Hz.

Steady state inactivation curves were measured from a holding potential of -80mV. A conditioning prepuls varying between -100 and 50mV in 10mV or 20mV increments was followed by a 20ms return to the holding potential and a 300ms test pulse to the maximum activation voltage (V_{max}). For Ca_v1.2 β 1 the prepuls duration was 5s, for Ca_v1.4 α 1 it was 5, 10, 20 or 30s to achieve a steady state. Pulse frequency was adapted to the prepuls duration and varied between 0.1 and 0.025Hz.

The effects of agonists and antagonists on Ca_v1.4 α 1 were tested by applying 40ms voltage pulses to V_{max} from a holding potential of -80mV or -50mV. Pulse frequency was 0.2Hz. Drug effects were measured after steady state block was attained, 2-3min after application.

2.5.3 *Data Analysis*

All values are given as mean \pm SEM, n is the number of experiments. An unpaired t test was performed for the comparison of two groups. Significance was tested by ANOVA followed by a Dunett test if multiple comparisons were made. Values of P<0.05 were considered significant.

To obtain current densities, the maximum current amplitude at maximum activation voltage (V_{max}) was normalized to the cell membrane capacitance (C_m).

Activation threshold, determined from I-V curves, is defined as the potential at which 5% of the maximum current were activated.

To determine the half maximum activation voltage ($V_{0.5, act}$) I-V curves were measured and the chord conductance (G) was calculated by dividing the peak current amplitude (I_{max}) by its

driving force at the respective test potential. The driving force is determined as the difference between the test potential (V_m) and the reversal potential (V_{rev}), the potential at which the I-V curve intersects with the x-axis. $G = I_{max} / (V_m - V_{rev})$. The chord conductance then was fitted by the Boltzmann equation $G = G_{max} / (1 + \exp(V_{0.5, act} - V_m) / k_{act})$, where G_{max} is the maximum conductance, V_m is the test potential and k_{act} is the slope factor of the activation curve.

To determine the half maximum inactivation voltage ($V_{0.5, inact}$) steady state inactivation curves were measured. Tail currents at maximum activation voltage (V_{max}) were normalized to the maximum current and plotted as a function of the preceding membrane potential of the conditioning pulse. Data points were fitted using the following Boltzmann function: $I = 1 / (1 + \exp(V_m - V_{0.5, inact}) / k_{inact})$.

The time course of $Ca_v1.2b\alpha1$ current activation was fitted by the monoexponential function: $I_t = A_0 * \exp(-t / \tau) + C$, where I_t is the current at time t after a voltage pulse to V_{max} , A_0 is the steady state current amplitude with the respective time constant of activation τ , and C is the remaining steady state current.

$Ca_v1.4\alpha1$ current activation was fitted by the biexponential function: $I_t = A_{fast} * \exp(-t / \tau_{fast}) + A_{slow} * \exp(-t / \tau_{slow}) + C$, where τ_{slow} and τ_{fast} represent slow and fast time constants of activation, respectively. A_{slow} and A_{fast} are the amplitudes of the current components.

The time course of current inactivation was fitted by the biexponential function: $I_t = A_{fast} * \exp(-t / \tau_{fast}) + A_{slow} * \exp(-t / \tau_{slow}) + C$. τ_{slow} and τ_{fast} represent slow and fast time constants of inactivation, respectively. A_{slow} and A_{fast} are the amplitudes of the current components. A_{fast} (%) was calculated as $A_{fast} / (A_{fast} + A_{slow}) * 100$. I_{Ba} of $Ca_v1.2b\alpha1$, 1.2-ICDI1.4 and 1.2 Δ C-ICDI1.4 were fitted by the monoexponential function $I_t = A_0 * \exp(-t / \tau) + C$, where A_0 is the steady state current amplitude with the respective time constant of inactivation τ , and C the remaining steady state current. For $Ca_v1.4\alpha1$, C1884Stop + ICDI, C1884Stop + CaM₁₂₃₄ and I_{Ba} of C1884Stop time course of inactivation was linear and therefore not fitted.

CDI was quantified by determining the f value. f is defined as the difference $r_{300, Ba} - r_{300, Ca}$, where r_{300} is the normalized current remaining after 300ms depolarization to the respective test potential (V_m) in the presence of Ba^{2+} and Ca^{2+} , respectively^{21,58}. f can vary between 0 (no CDI) and 1 (complete CDI). It was determined for test potentials between -40mV and 40mV in 10mV increments. For comparison of different channels the maximum f value was taken.

For generation of concentration-inhibition curves $I_{drug} / I_{control}$ was determined, where I_{drug} is the steady state current amplitude at V_{max} in the present and $I_{control}$ in the absence of the required substances (see 2.5.1). The drugs were tested at 4-5 different concentrations. Data

points were fitted to the Hill equation. $1 / [1 + (IC_{50} / c)]^{n_H}$, c is the drug concentration, n_H is the Hill coefficient and IC_{50} is the drug concentration needed for half maximum block of $I_{control}$.

3 RESULTS

3.1 Functional characterization of $\text{Ca}_v1.4\alpha1$

The $\text{Ca}_v1.4\alpha1$ subunit was cloned from murine retinal cDNA. For these purposes specific primer pairs based on the previously published sequence of this channel⁵⁹ were designed (see appendix 6.3) and RT-PCR with retinal cDNA from mouse strain C57Bl6 was performed. The full-length cDNA of $\text{Ca}_v1.4\alpha1$ was determined to be 6111 bp with an open reading frame encoding a protein of 1984 amino acid residues (sequence see appendix 6.1, GenBank accession number: AJ579852). In the context of this work detailed electrophysiological experiments were performed to characterize $\text{Ca}_v1.4$ channels biophysically and pharmacologically.

3.1.1 Electrophysiological properties of wild type *Cav1.4*

HEK 293 cells were transfected with $\text{Ca}_v1.4\alpha1$ without any auxiliary subunits or the empty pIRES2-EGFP expression vector for measurement of endogenous HEK cell currents as control. In both cases only endogenous HEK cell currents⁶⁰ were observed.

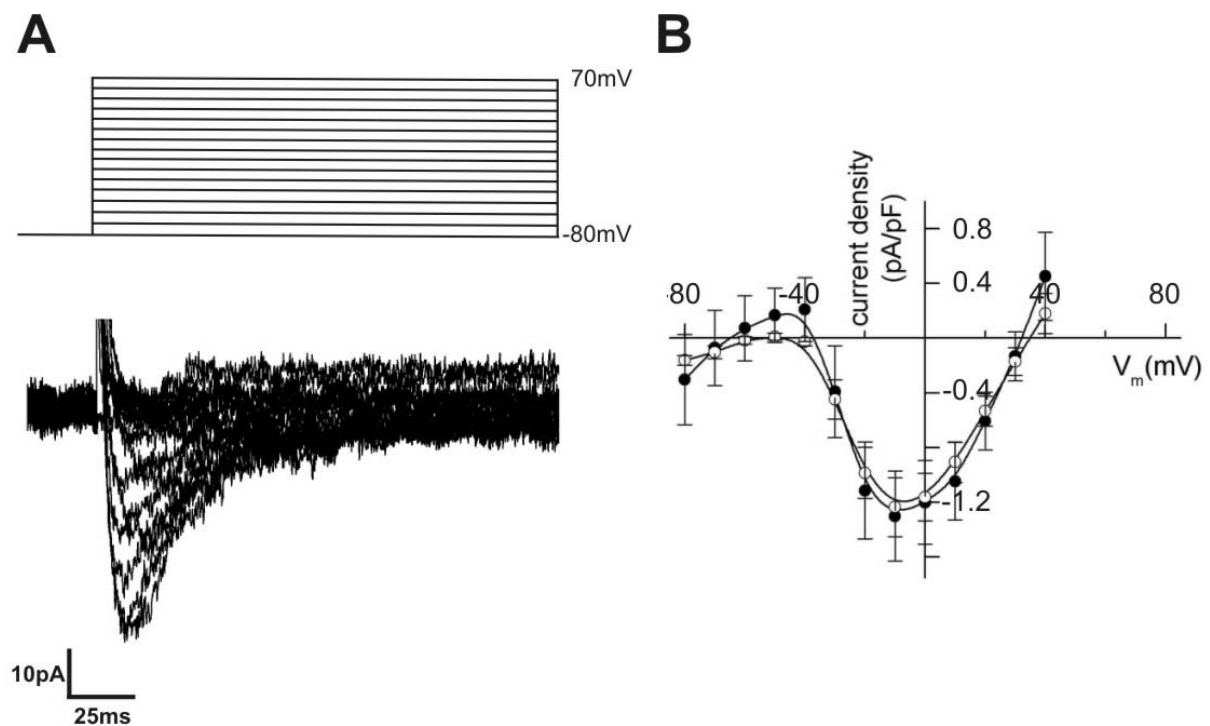


Figure 3-1 HEK 293 cells were transfected with empty pIRES2-EGFP expression vector or $\text{Ca}_v1.4\alpha1$. Currents were measured in bath solution containing 30mM Ba^{2+} . There was no difference between endogenous current and $\text{Ca}_v1.4\alpha1$ current. **A, top)** Pulse protocol: 150ms voltage pulses were applied from a holding potential of -80mV to potentials between -80 and 70mV in 10mV increments. **A, bottom)** Whole cell current recorded from a representative cell. **B)** I-V relationship for cells transfected with $\text{Ca}_v1.4\alpha1$ (○, $n = 12$) and pIRES2-EGFP (●, $n = 7$). Current densities at V_{max} were $-1.2 \pm 0.2\text{pA/pF}$ for $\text{Ca}_v1.4\alpha1$ and -1.3 ± 0.3 pA/pF for pIRES2-EGFP.

There was no difference either in current density or in the I-V relationship (Figure 3-1) suggesting that $\text{Ca}_v1.4\alpha1$ is not able to form functional LTCCs alone. Perhaps other calcium channel subunits are needed for formation of functional LTCCs. Indeed, when coexpressed with $\alpha2\delta$ and either $\beta2a$ or $\beta3$ subunits Ba^{2+} currents completely different from endogenous background currents were evoked by depolarizations (Figure 3-2). The I-V relationship was shifted 20mV to more positive potentials and current densities consistently exceeded those of endogenous currents. Furthermore, no significant inactivation was seen during the 150ms voltage step (Figure 3-2).

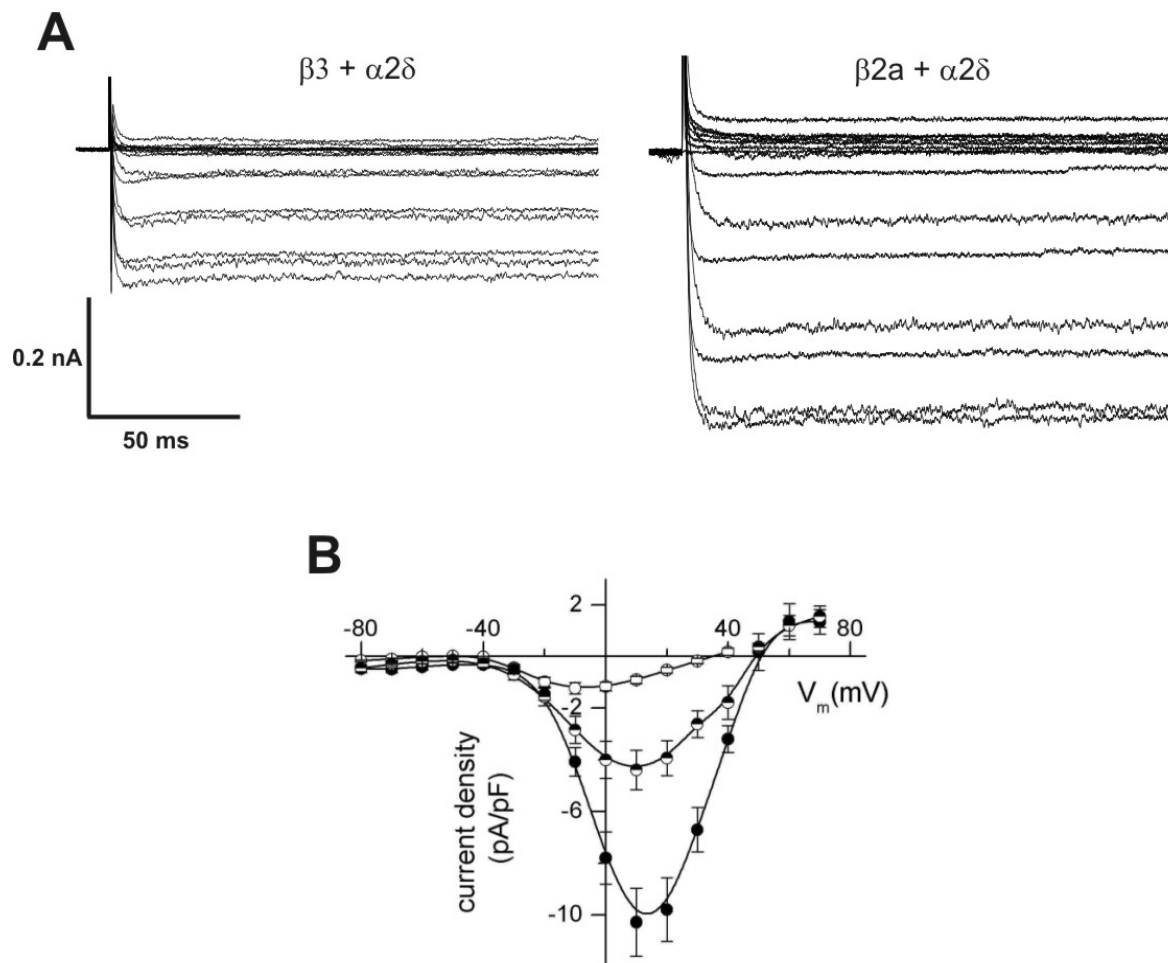


Figure 3-2 HEK 293 cells were transfected with $\text{Ca}_v1.4\alpha1$, $\alpha2\delta1$ and $\beta3$ or $\beta2a$ subunit or with $\text{Ca}_v1.4\alpha1$ alone. Currents were measured in bath solution containing 30mM Ba^{2+} . Same pulse protocol was used as in Figure 1. **A**) Current amplitudes recorded with $\beta2a$ subunits were bigger than with $\beta3$ subunits at comparable cell capacity. **B**) The I-V relationship was shifted about 20mV to more positive potentials for heterologously expressed currents compared with endogenous HEK cell currents. V_{max} was -6.7 ± 1.4 for $\text{Ca}_v1.4\alpha1$ alone (\circ , $n = 12$), 11.0 ± 1.8 mV for $\beta3$ subunit (\bullet , $n = 10$) and 13.8 ± 0.9 mV for $\beta2a$ subunit (\bullet , $n = 30$). Current densities were -1.2 ± 0.2 pA/pF for endogenous currents (\circ , $n = 12$), -4.4 ± 0.8 pA/pF for $\beta3$ subunit (\bullet , $n = 10$) and -9.5 ± 1.1 pA/pF for $\beta2a$ (\bullet , $n = 30$). See also table 3-1.

Two different β subunits for heterologous expression of $\text{Ca}_v1.4$ were tested, the $\beta2a$ and the $\beta3$ subunit. The properties of the currents obtained from both experiments were very similar (Table 3-1). As the only difference the current density recorded with the $\beta2a$ subunit coexpressed was two times the current density recorded with the $\beta3$ subunit (Figure 3-2).

Based on these findings, the $\beta2a$ subunit was used for heterologous expression of $\text{Ca}_v1.4$ and $\text{Ca}_v1.2$ calcium channels for all further experiments. To describe the biophysical properties of $\text{Ca}_v1.4$ more exactly it was compared with $\text{Ca}_v1.2b$, the smooth muscle isoform of LTCCs, which is well characterized. Ba^{2+} currents of $\text{Ca}_v1.4$ apparently activated faster than Ba^{2+} currents of $\text{Ca}_v1.2$ (Figure 3-3A, Table 3-1). Consistent with the properties of an LTCC, $\text{Ca}_v1.4$ activated at relatively positive membrane potentials. In experiments performed with 30 mM Ba^{2+} as the charge carrier, the mean I–V relationships of $\text{Ca}_v1.4$ and $\text{Ca}_v1.2$ were almost identical (Figure 3-3B, Table 3-1). Only the inactivation kinetics of $\text{Ca}_v1.4$ were completely different from those of $\text{Ca}_v1.2$. During a 150ms voltage pulse applied (Figure 3-3A) no inactivation could be observed at all. For comparison of voltage dependent activation and inactivation (VDI), activation and steady state inactivation curves of Ba^{2+} currents were determined. Activation curves were almost identical for $\text{Ca}_v1.2$ and $\text{Ca}_v1.4$. In contrast, at a conditioning pulse duration of 5s (2.5.2) the steady state inactivation curve of $\text{Ca}_v1.4$ was shifted to approximately 20mV more positive membrane potentials compared to $\text{Ca}_v1.2$ (Figure 3-3C). At V_{max} it took more than 30s for complete inactivation of $\text{Ca}_v1.4$ Ba^{2+} currents (Figure 3-4).

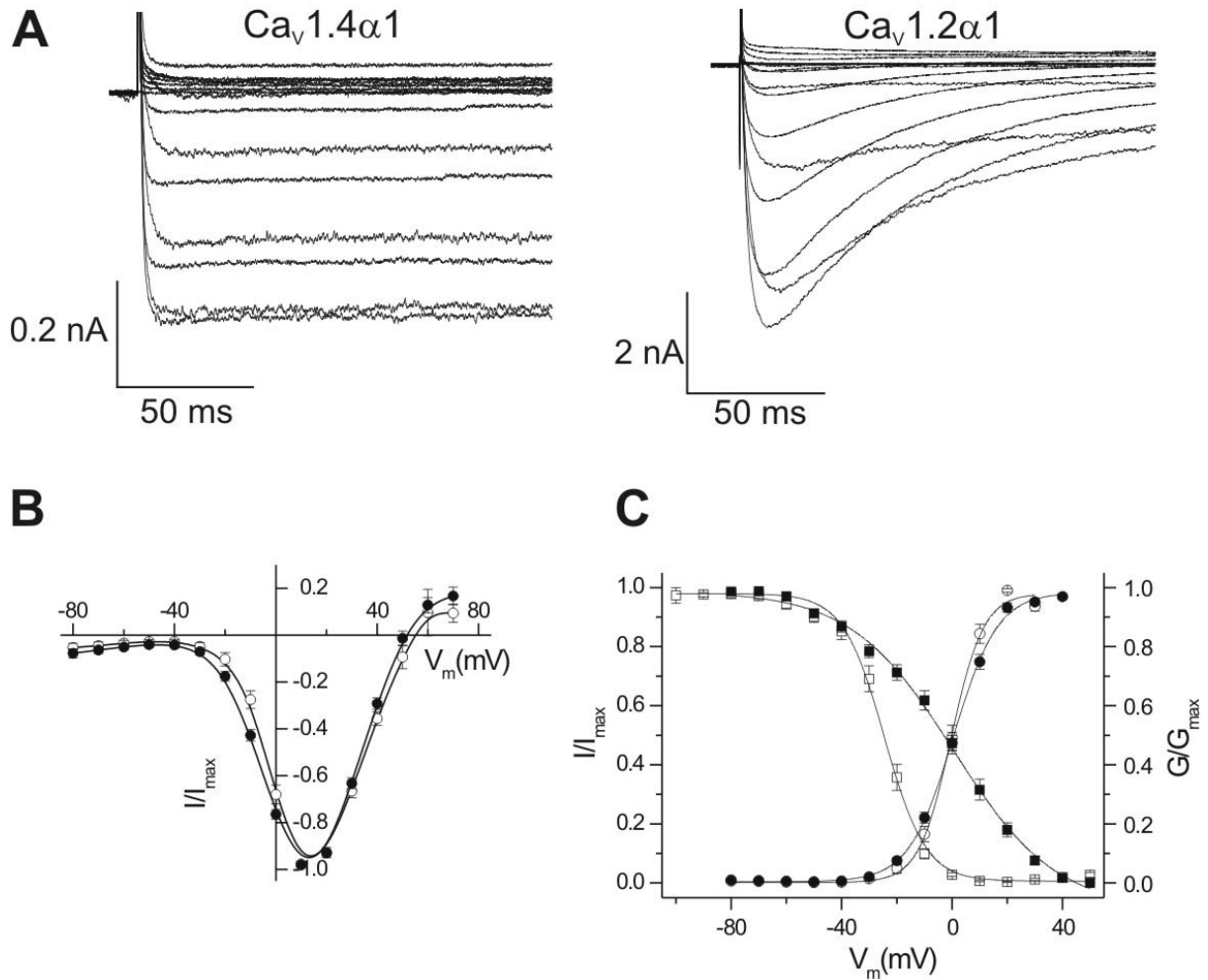


Figure 3-3 $Ca_v1.4$ induces L-type Ba^{2+} currents in HEK293 cells. For all experiments $Ca_v1.4\alpha1$ or $Ca_v1.2\alpha1$ were coexpressed with $\alpha2\delta1$ and $\beta2a$. Currents were measured in bath solution containing 30 mM Ba^{2+} as the charge carrier. Pulse protocol as given in Figure 1. Biophysical parameters are given in table 3-1. **A**) Whole-cell current recorded from representative cells expressing either $Ca_v1.4$ (left) or $Ca_v1.2$ (right). **B**) I-V relationship for $Ca_v1.4$ channels (\bullet , $n = 30$) and $Ca_v1.2$ channels (\circ , $n = 9$). Individual I-V curves were normalized to the respective maximum current amplitude and then averaged. **C**) Conductance-voltage relationships for $Ca_v1.4$ (\bullet , $n = 28$) and $Ca_v1.2$ (\circ , $n = 9$) and steady state inactivation curves for $Ca_v1.4$ (\blacksquare , $n = 9$) and $Ca_v1.2$ (\square , $n = 9$) were determined. Individual curves were normalized to maximum current amplitude and then averaged. *Solid lines*: datafit to the Boltzmann equation.

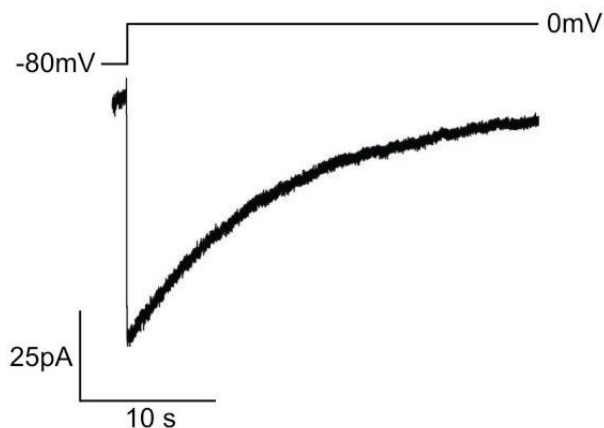


Figure 3-4 Representative Ba^{2+} current of a cell expressing heterologous $Cav1.4$ channels. More than 30s depolarization to V_{max} are needed for full inactivation. Pulse protocol see above.

Because of the extreme slow inactivation time course of $\text{Ca}_v1.4 \text{ Ba}^{2+}$ currents, the duration of the conditioning pulse for measurement of VDI was modified. It was set 5, 10, 20 and 30s. The inactivation curves were shifted to more hyperpolarized voltages and the slope of the inactivation curve decreased with increasing prepuls duration (Figure 3-5). There was no significant difference between the inactivation curves left for 20 and 30s prepuls duration, indicating the achievement of a steady state after a 20s conditioning pulse.

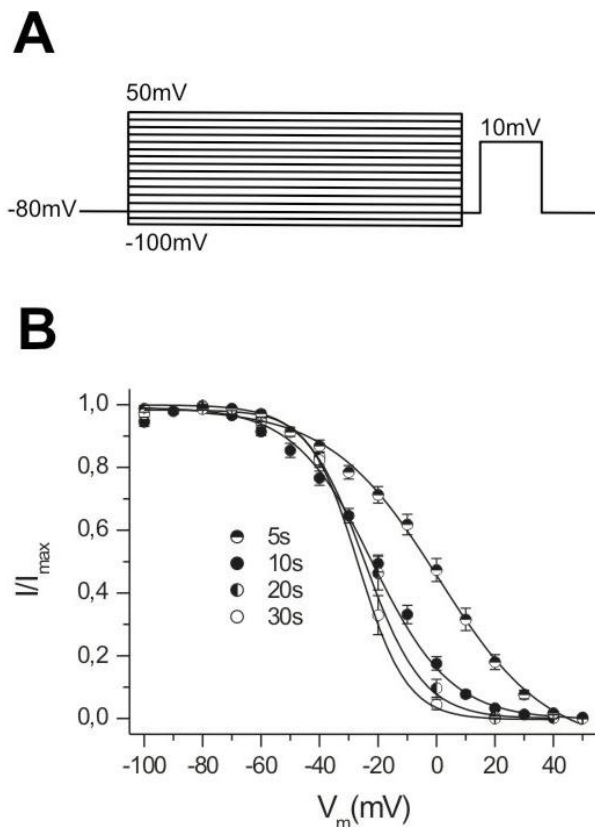


Figure 3-5 Dependence of voltage dependent inactivation of $\text{Ca}_v1.4$ on prepuls duration. Bath solution containing 30mM Ba^{2+} was used for measurements. **A)** Pulse protocol for measurement of inactivation curves. From a holding potential of -80mV a conditioning prepulse of variable length to potentials between -100 and 50mV was applied. After a 20ms return to the holding potential the cells were clamped to 10mV (V_{max}) for 300ms. **B)** Parameters obtained from inactivation curves:

| | |
|---------------|--|
| 5s prepulse: | $V_{0.5,\text{inact}} = 0.64 \pm 2.6\text{mV}$, $k_{\text{inact}} = 17.5 \pm 0.8\text{mV}$, $n = 9$; |
| 10s prepulse: | $V_{0.5,\text{inact}} = -20.1 \pm 1.6\text{mV}$, $k_{\text{inact}} = 14.5 \pm 1.0\text{mV}$, $n = 8$; |
| 20s prepulse: | $V_{0.5,\text{inact}} = -21.4 \pm 2.1\text{mV}$, $k_{\text{inact}} = 10.1 \pm 1.0\text{mV}$, $n = 7$; |
| 30s prepulse: | $V_{0.5,\text{inact}} = -25.7 \pm 1.9\text{mV}$, $k_{\text{inact}} = 8.1\text{mV} \pm 0.6$, $n = 6$. |

In vivo, the permeating ion of LTCCs is Ca^{2+} , not Ba^{2+} . Ca^{2+} plays a major key role in their inactivation. This is of great importance for the normal physiological function of LTCCs. Ca^{2+} characteristically accelerates the time course of current inactivation. Surprisingly, current traces of $\text{Ca}_v1.4$ with 10mM Ba^{2+} and 10mM Ca^{2+} , respectively, show identical kinetics. Thus, unlike in $\text{Ca}_v1.2$ channels, Ca^{2+} does not accelerate inactivation in $\text{Ca}_v1.4$ channels⁶¹. Only current density was reduced by $30.1 \pm 0.03\%$ ($n = 9$) in comparison to the Ba^{2+} current and the I-V relationship was shifted approximately 10mV to more positive membrane potentials without affecting the slope of activation and inactivation curves (Figure 3-6).

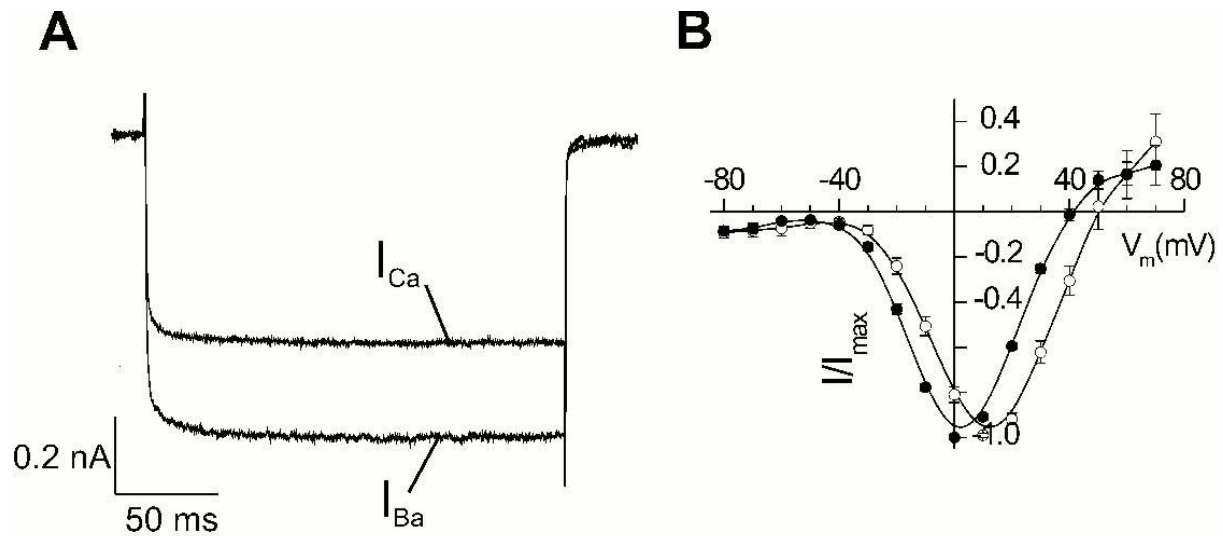


Figure 3-6 HEK 293 cells were transfected with $Ca_v1.4\alpha1$, $\beta2a$ and $\alpha2\delta$ subunits. Currents were recorded with either 10mM Ca^{2+} (I_{Ca}) or Ba^{2+} (I_{Ba}) as charge carrier. From a holding potential of $-80mV$ a test pulse to 10mV was applied for 150ms at 0.2 Hz. I_{Ca} and I_{Ba} were measured from the same cell. **A)** Current traces from a representative cell. No inactivation was observed in both cases. **B)** Normalized I-V relationship for I_{Ca} (\circ , $n=9$) and I_{Ba} (\bullet , $n=16$). Data see table 3-1.

Table 3-1 Biophysical properties of I_{Ba} and I_{Ca} from heterologously expressed $Ca_v1.4$ and $Ca_v1.2$ channels

| Subunits coexpressed with $\alpha2\delta1$ | Charge carrier (mM) | $V_{0.5,act}$ (mV) | k_{act} (mV) | V_{max} (mV) | Activation threshold (mV) | $V_{0.5,inact}$ (mV) | k_{inact} (mV) |
|--|--|-----------------------------|----------------------------|------------------------------|-----------------------------|-----------------------------|--------------------------|
| $Ca_v1.2\beta\alpha1 + \beta2a$ | 30 Ba^{2+} | -0.1 ± 1.2 $n=9$ | $5.6 \pm 0.4^*$ $n=9$ | 13.3 ± 1.7 $n=9$ | -23.4 ± 1.9 $n=9$ | $-24.3 \pm 1.5^*$ $n=9$ | $6.8 \pm 0.7^*$ $n=9$ |
| $Ca_v1.4\alpha1 + \beta2a$ | 30 Ba^{2+} | 1.12 ± 1.0 $n=28$ | 7.92 ± 0.22 $n=28$ | 13.8 ± 0.9 $n=30$ | -28.0 ± 1.2 $n=30$ | 0.64 ± 2.6 $n=9$ | 17.5 ± 0.8 $n=9$ |
| $Ca_v1.4\alpha1 + \beta2a$ | 30 Ba^{2+} + 1 μM BayK 8644 | $-7.8 \pm 7.2^*$ $n=5$ | $4.66 \pm 0.8^*$ $n=5$ | $-4 \pm 4^*$ $n=5$ | -32.7 ± 1.8 $n=5$ | n.d. | n.d. |
| $Ca_v1.4\alpha1 + \beta2a$ | 10 Ba^{2+} | $-12.0 \pm 0.8^*$ $n=16$ | $6.32 \pm 0.1^*$ $n=16$ | $-0.9 \pm 0.7^*$ $n=16$ | $-37.8 \pm 1.1^*$ $n=16$ | $-27.1 \pm 2.6^*$ $n=8$ | 15.1 ± 0.8 $n=8$ |
| $Ca_v1.4\alpha1 + \beta2a$ | 10 Ca^{2+} | $-1.1 \pm 1.8^\#$ $n=9$ | $8.1 \pm 0.4^\#$ $n=9$ | $11.1 \pm 1.1^\#$ $n=9$ | $-29.7 \pm 1.0^\#$ $n=9$ | $-15.4 \pm 1.7^\#$ $n=8$ | 17.0 ± 1.5 $n=8$ |
| $Ca_v1.4\alpha1 + \beta3$ | 30 Ba^{2+} | 0.74 ± 2.5 $n=10$ | $10.4 \pm 1.0^*$ $n=10$ | 11.0 ± 1.8 ($n=10$) | $-37.2 \pm 2.4^*$ $n=10$ | n.d. | n.d. |

n.d.: not determined. Statistical differences for $V_{0.5,act}$, k_{act} , V_{max} , activation threshold, $V_{0.5,inact}$ and k_{inact} are given in comparison to $Ca_v1.4\alpha1$ and $\beta2$ with 30mM Ba^{2+} (*, $P<0.05$) or 10mM Ba^{2+} ($^\#$, $P<0.05$) as the charge carrier.

3.1.2 Pharmacological properties of wild type $Ca_v1.4\alpha1$

To study the pharmacological profile of heterologously expressed $Ca_v1.4$ channels, the blocking effect of different calcium channel antagonists was tested. The dihydropyridine (DHP) isradipine blocked I_{Ba} at a holding potential of -80mV with an IC_{50} of $200 \pm 50\text{nM}$ ($n = 5-9$, Figure 3-7). At a holding potential of -80mV , 100nM isradipine blocked $41.9 \pm 0.03\%$ ($n = 7$) of I_{Ba} . Changing the holding potential to -50mV significantly increased the block to $88.3 \pm 0.01\%$ ($n = 9$) of I_{Ba} , indicating a strong voltage-dependence of the observed block (Figure 3-7). $Ca_v1.4$ was only weakly sensitive to verapamil. At a holding potential of -80mV , $100\mu\text{M}$ verapamil blocked $69.1 \pm 0.13\%$ ($n = 5$) of I_{Ba} . Also, the two enantiomers of Diltiazem were tested under identical conditions. Surprisingly, their concentration-response relationships were not significantly different from each other (Figure 3-7). L-cis-diltiazem blocked I_{Ba} with an IC_{50} of $74.8 \pm 8.3\mu\text{M}$ ($n = 4-6$), and D-cis-diltiazem blocked I_{Ba} with an IC_{50} of $91.6 \pm 9.4\mu\text{M}$ ($n = 4-6$). Normally, for typical LTCCs, the affinity of L-cis-diltiazem is several orders of magnitude lower than that of D-cis-diltiazem⁶². Finally, a DHP receptor agonist, S(-)-Bay K8644, was tested on $Ca_v1.4$ channels. At a concentration of $1\mu\text{M}$, it increased the current density of I_{Ba} approximately sixfold. As in other LTCCs, BayK 8644 shifted the I-V relationship approximately 8-10mV to more hyperpolarized potentials (Figure 3-7, table 3-1).

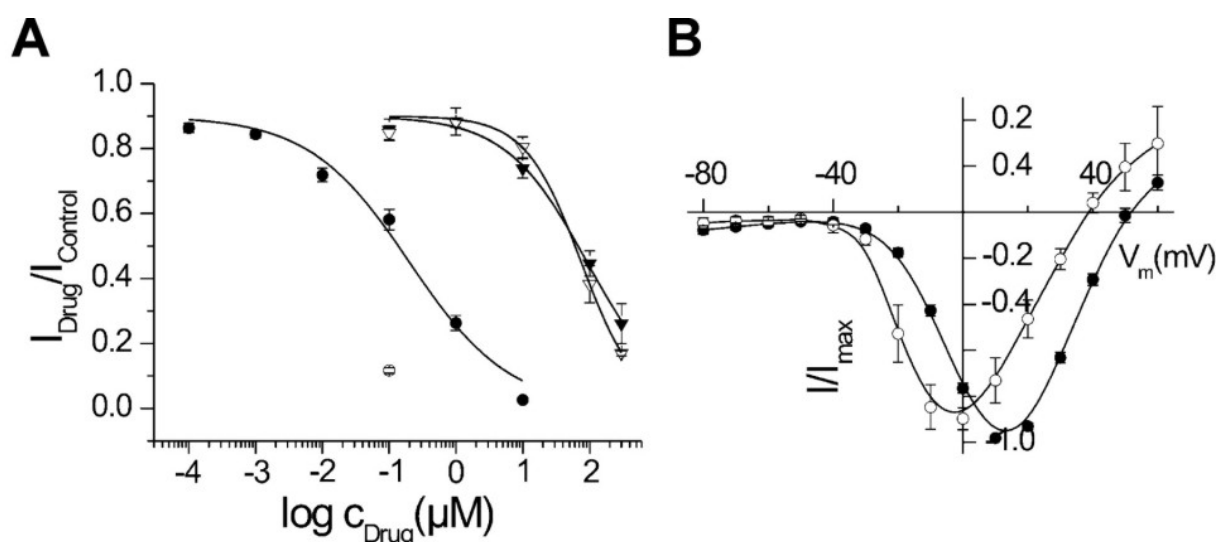


Figure 3-7 Sensitivity of $Ca_v1.4$ channels for LTCC blockers and S(-)-Bay K8644. For all experiments $Ca_v1.4\alpha1$ was coexpressed with $\alpha2\delta1$ and $\beta2a$. Currents were measured in bath solution containing 30mM Ba^{2+} as the charge carrier. **A**) Concentration-response curves for inhibition of $Ca_v1.4$ by D-cis-diltiazem (∇ , $n = 5-6$), L-cis-diltiazem (\blacktriangledown , $n = 5-6$), and isradipine (\bullet , $n = 5-9$). Pronounced voltage dependence of isradipine block was observed when the holding potential was changed from -80mV to -50mV (\circ , $n = 9$). **B**) I-V relationship for $Ca_v1.4$ in the absence (\bullet , $n = 30$) and presence of $1\mu\text{M}$ S(-)-Bay K8644 (\circ ; $n = 5$).

3.2 The lack of calcium dependent inactivation (CDI)

A typical LTCC showing CDI is $Ca_v1.2b$, the smooth muscle isoform. In the presence of Ba^{2+} as charge carrier inactivation is relatively slow and solely affected by membrane potential (VDI). When Ca^{2+} is the permeating ion $Ca_v1.2$ inactivates much faster as a result of CDI (Figure 3-8A). This effect is quantified by calculating the f value, which is the difference of normalized I_{Ba} and I_{Ca} remaining after 300ms depolarization. Characteristically, the f value shows a U-shaped dependence on the membrane potential²¹. Our experiments reveal a maximum f value (f_{max}) of about 0.3 for $Ca_v1.2$ and this U-shaped dependence of f (Figure 3-8B). For $Ca_v1.4$ the normalized current traces for I_{Ba} and I_{Ca} are congruent, there is no difference in terms of kinetics (Figure 3-8C). f_{max} is not significantly different from zero over the whole voltage range (Figure 3-8D).

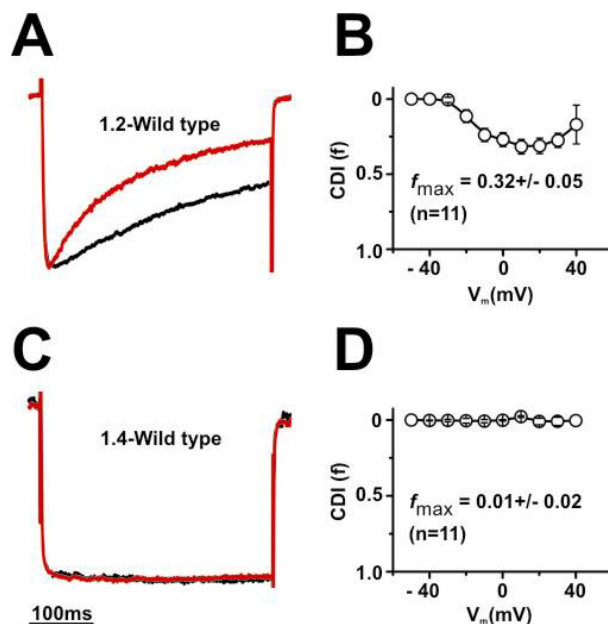


Figure 3-8 $Ca_v1.4$ channels completely lack CDI. All current traces were measured at $V_m = 10mV$ from a holding potential of $-80mV$ and normalized to maximum current amplitude. Pulse duration was 300ms. Kinetic parameters for wild type channels are given in table 3-2. **A,C**) Representative traces of I_{Ba} (black) and I_{Ca} (red) for $Ca_v1.2$ (A) and $Ca_v1.4$ (C), respectively. **B,D**) Voltage dependence of f for $Ca_v1.2$ (B) and $Ca_v1.4$ (D). f_{max} is the maximum f value, n is the number of cells.

3.2.1 Calmodulin binding of $Ca_v1.4\alpha1$

An explanation why $Ca_v1.4$ is lacking CDI could be that it cannot bind calmodulin. The alignment of $Ca_v1.4\alpha1$ and $Ca_v1.2b\alpha1$ shows that the region coding for the whole calcium sensing apparatus is principally conserved. However, there are some amino acid exchanges in the Pre-IQ region that could affect the affinity of calmodulin (Figure 1-5). To test for this option GST pull-down assays were performed with GST fusion proteins containing the whole C-terminus or the proximal or the distal part of the C-terminus of $Ca_v1.4\alpha1$ and $Ca_v1.2b\alpha1$, respectively. Calmodulin binding was observed to the full length C-terminus of $Ca_v1.2b\alpha1$ (CT1.2) and of $Ca_v1.4\alpha1$ (CT1.4) in the presence, but not in the absence of calcium

(Figure 3-9B). For control of expression and molecular weight, 25pmol of each GST fusion protein were blotted and detected with an anti-GST antibody (Figure 3-9C).

Calmodulin is known to bind to the proximal part of the C-terminus of $Ca_v1.2\beta\alpha1$ ^{17,21-28}. Due to this fact it was tested if it binds to the corresponding region in $Ca_v1.4\alpha1$. CT1.2-1667Stop and CT1.4-1610Stop displayed calmodulin binding in a calcium dependent manner (Figure 3-9D, lanes 1-4). No binding of calmodulin was observed to the distal part of the C-termini of $Ca_v1.2$ (CT1.2 1667-2166) and $Ca_v1.4$ (CT1.4 1610-1984) (Figure 3-9D, lanes 5-8). Expression of the fusion proteins was again tested by western blot (Figure 3-9E).

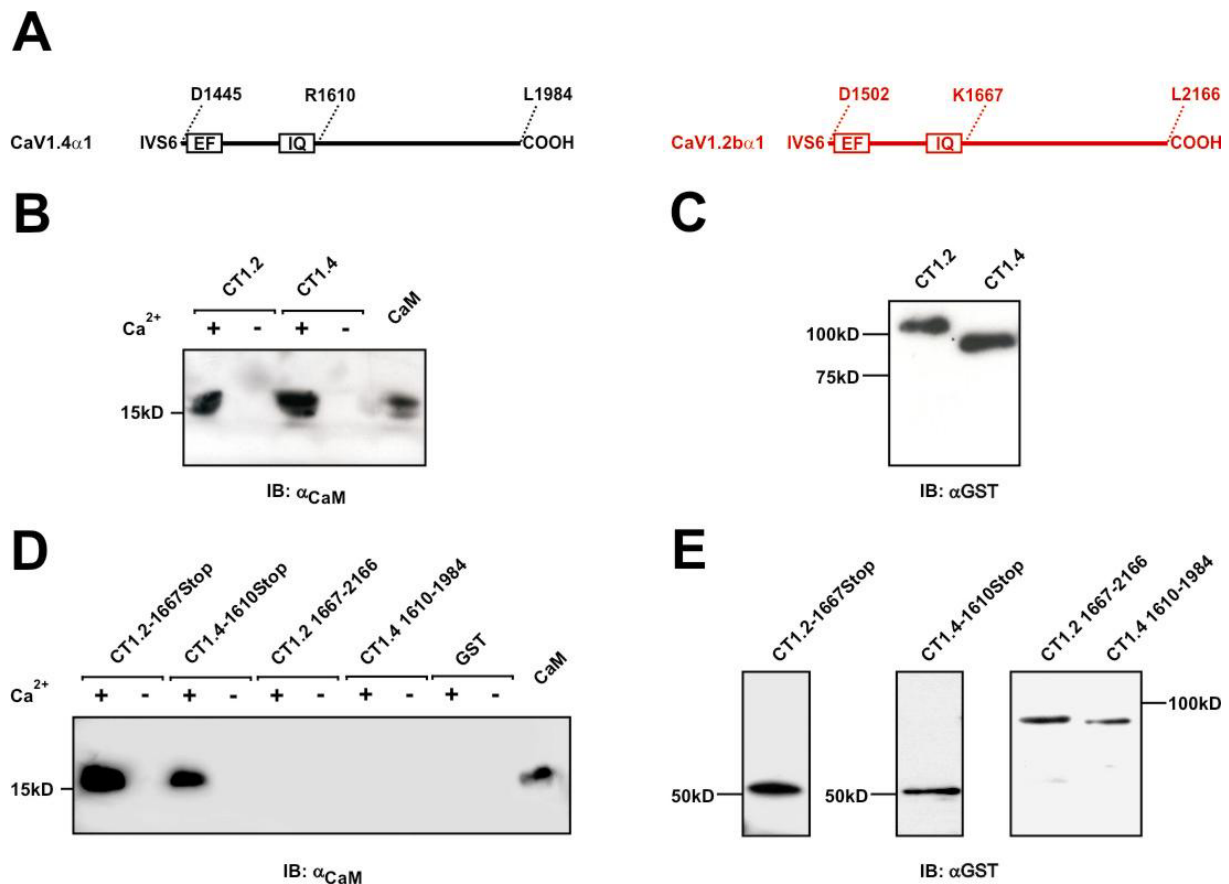


Figure 3-9 Calmodulin binding of $Ca_v1.4\alpha1$. Each experiment was repeated at least three times. **A**) Scheme of $Ca_v1.4\alpha1$ (left) and $Ca_v1.2\beta\alpha1$ cytosolic C-termini (right). **B**) GST pull-down with the full length C-termini (CT1.2, 105kDa and CT1.4, 95kDa) and calmodulin in the presence (+) and in the absence (-) of Ca^{2+} . Ca^{2+} dependent binding of calmodulin (17kDa) was observed for $Ca_v1.4\alpha1$ and $Ca_v1.2\beta\alpha1$. 1μg calmodulin was blotted as control (last lane). For detection an anti-calmodulin antibody was used. **C**) Western blot for control of expression of the GST fusion proteins comprising the whole C-terminus. For detection an anti-GST antibody was used. 25pmol of each protein were blotted. **D**) Same GST pull-down assay was performed as in 9B, using fusion proteins containing fragments corresponding to the proximal (CT1.2-1667Stop, 51kDa and CT1.4-1610Stop, 51kDa) and the distal parts (CT1.2 1667-2166, 85kDa and CT1.4 1610-1984, 73kDa) of the C-termini of $Ca_v1.2\beta\alpha1$ and $Ca_v1.4\alpha1$, respectively. As a negative control GST was used. **E**) Control of expression of the fusion proteins by Western blot. Performance see panel C.

3.2.2 *Identification of an inhibitory channel domain*

Considering these results the lack of CDI cannot be caused by the inability of calmodulin to bind to the channel. These findings rather suggest that Ca_v1.4 harbors an inhibitory domain that is able to mask CDI and this domain should reside downstream of the IQ motif in the distal C-terminus. To check these assumptions several mutant Ca_v1.4 α 1 subunits were constructed with the distal C-terminus truncated at different positions (2.1.1.1, Figure 3-10A). In every mutant the whole Ca²⁺ sensing machinery was left functional. Mutant C1884Stop showed fast inactivation in the presence of Ca²⁺ in electrophysiological experiments. CDI was fully recovered with an f_{\max} of about 0.3 like in Ca_v1.2 channels and the typically U-shaped voltage dependence of f . (Figure 3-10B, C, F, table 3-2). Also mutants R1610Stop, Y1668Stop and R1796Stop showed CDI to the same extent as Ca_v1.2 channels (Figure 3-10F, table 3-2). The kinetic parameters for all these truncation mutants showing CDI were in the same range as for Ca_v1.2 wild type channels.

The next step was the coexpression of the C1884Stop mutant with a negative dominant calmodulin mutant (CaM₁₂₃₄) that can bind to the C-terminus but is deficient for Ca²⁺ binding and thus cannot mediate CDI⁴⁸. In these experiments no CDI was observed (Figure 3-10D, F, table 3-2). Furthermore, C1884Stop was coexpressed with the peptide corresponding to amino acids 1885-1984 of Ca_v1.4 α 1 (inhibitor of CDI, ICDI). Again no CDI was present at all (Figure 3-10E, F, table 3-2). For the Δ C mutant in which the ICDI domain was directly attached to the IQ motif no CDI was seen either (Figure 3-10F, table 3-2). To narrow down the sequence important to prevent CDI two other mutants were constructed. Q1930Stop showed full CDI like the other truncation mutants whereas Q1953Stop behaved like wild type Ca_v1.4 (Figure 3-10F, table 3-2).

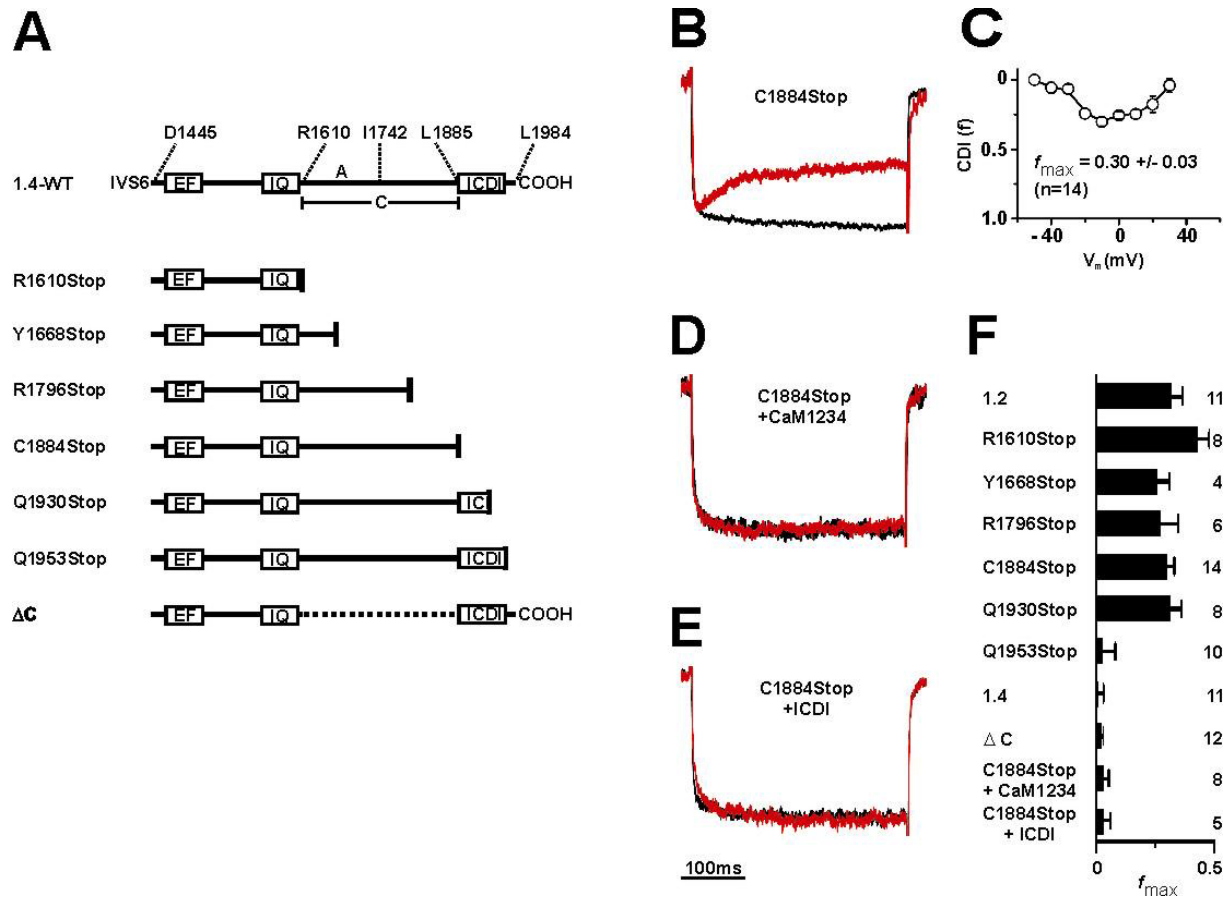


Figure 3-10 An inhibitory domain prevents CDI in $Ca_v1.4$ channels. Currents were measured as mentioned in Figure 8. Kinetic parameters for all constructs are given in table 3-2. **A)** Schematic representation of constructed $Ca_v1.4\alpha1$ mutants. Deletions are marked by dotted lines. **B)** Representative traces of I_{Ba} (black) and I_{Ca} (red) for mutant C1884Stop. **C)** Voltage dependence of f for C1884Stop. f_{max} is the maximum f value, n is the number of cells. **D,E)** Representative current traces for C1884Stop coexpressed with CaM_{1234} and ICDI, respectively. No CDI was observed in both cases. **F)** f_{max} values for wild type channels, mutant channels and coexpression experiments. Number of cells is indicated at the right side.

3.2.3 Interaction of ICDI and $Ca_v1.4\alpha1$

The next question was how ICDI interacts with $Ca_v1.4\alpha1$. To clarify this issue coimmunoprecipitations were performed. To this end different C-terminal fragments of $Ca_v1.4\alpha1$ were fused with a N-terminal myc tag and the ICDI domain was equipped with a N-terminal triple flag tag (Figure 3-11A). ICDI bound to the proximal C-terminus of $Ca_v1.4\alpha1$ (CT1.4-1610Stop, Figure 3-11B, lane 4, upper panel) as supposed. Binding was no longer observed when the EF-hand was deleted in the proximal C-terminus (ΔEF , 3-Figure 11B, lane 5, upper panel). No binding was observed either between ICDI and peptide C or peptide A (Figure 3-11C, lane 4 and 5, lower panel). Expression of all fusion proteins was again tested by western blot (Figure 3-11C).

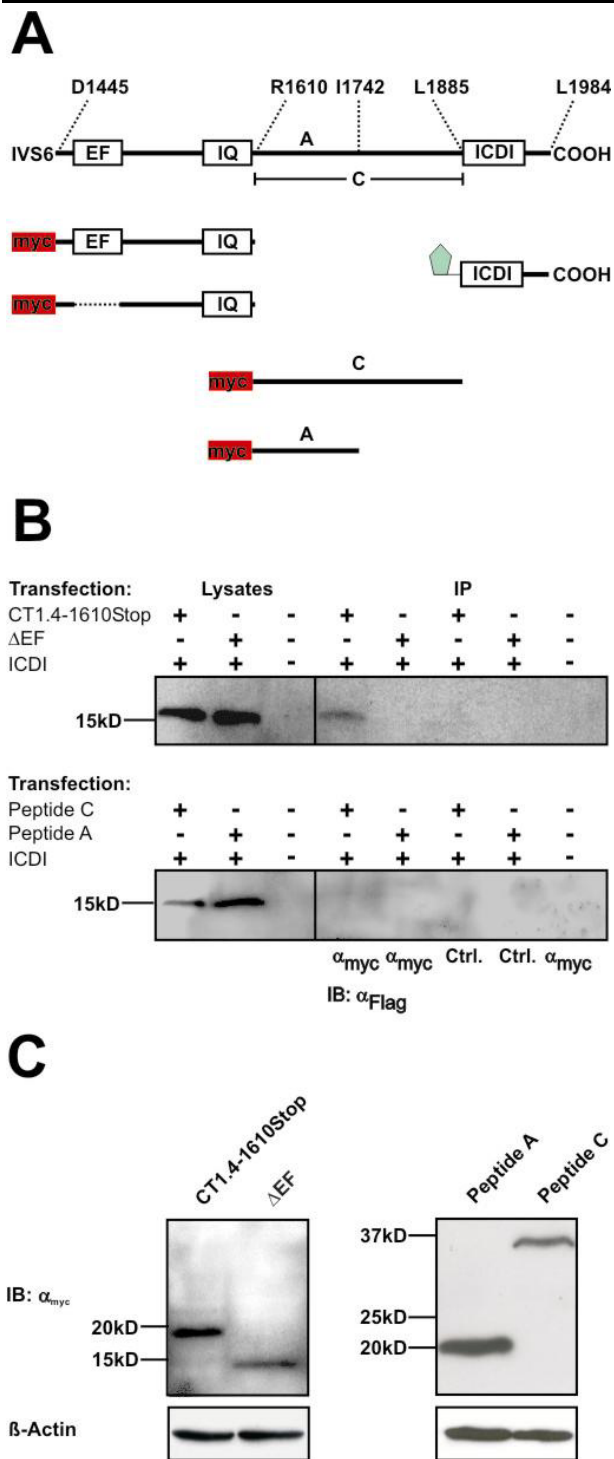


Figure 3-11 Interaction of ICDI domain and the C-terminus of $Ca_v1.4\alpha1$. **A)** Schematic representation of the C-terminus of $Ca_v1.4\alpha1$ starting after the IVS6 segment. The amino acid numbers are the borders of peptide A, peptide C and ICDI.

B) Upper panel: Coimmunoprecipitation of HEK 293 cells coexpressing flag tagged ICDI and CT1.4-1610Stop or ΔEF . For control of expression of ICDI pure lysates of transfected and untransfected cells were blotted (lane 1-3). Precipitation was done with anti-myc antibody (lane 4 and 5) and with anti-ras antibody as a control (lane 6 and 7). Also untransfected cells were probed (lane 8).

Lower panel: Coimmunoprecipitation of HEK 293 cells coexpressing flag tagged ICDI and peptide C or peptide A. Conditions as mentioned in the upper panel. **3-11C)** Expression of myc tagged constructs in HEK 293 cells (CT1.4-1610Stop: 20kDa, ΔEF : 16kDa, peptide A: 16kDa, peptide C: 31kDa). β -Actin is shown as loading control

These findings were corroborated by a series of GST pull-down assays performed with GST fusion proteins comprising the same parts of the C-terminus of $Ca_v1.4\alpha1$ as the proteins for the coimmunoprecipitations. As the only difference the ICDI peptide was provided with a single flag tag. The results were the same as for the coimmunoprecipitations. ICDI binds to the proximal C-terminus of $Ca_v1.4\alpha1$, but not to the proximal C-terminus lacking the EF-hand motif. Binding to peptide A was not observed either (Figure 3-12A). Expression of the fusion proteins was confirmed by western blot (Figure 3-12B).

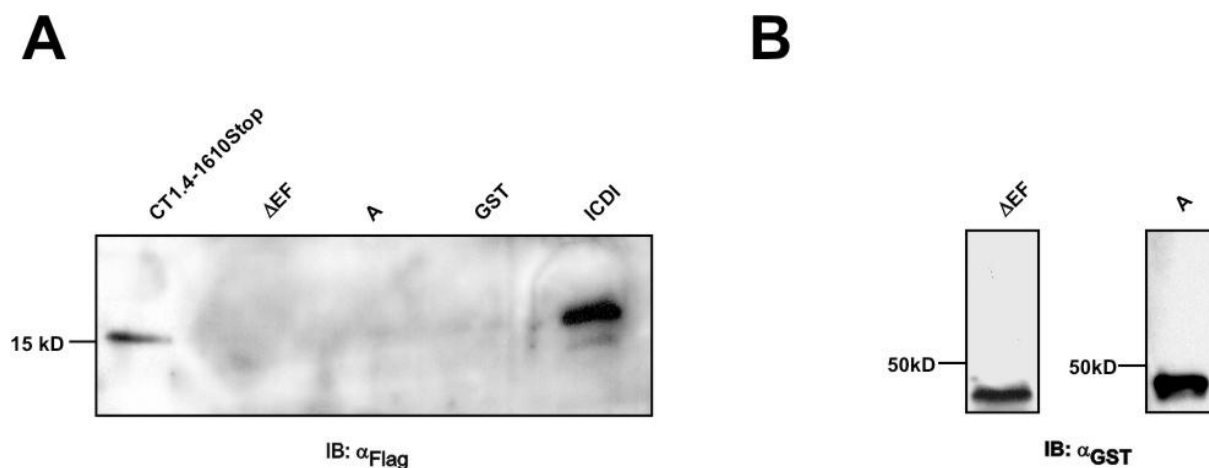


Figure 3-12 Interaction between ICDI domain and the C-terminus of $Ca_v1.4\alpha1$. **A)** GST pull-down with a fusion protein containing the proximal C-terminus of $Ca_v1.4\alpha1$ (CT1.4.1610Stop, lane 1), the same protein lacking the EF motif (Δ EF, lane 2) and a fusion protein containing peptide A (A, lane 3). As a negative control GST was used (GST, lane 4). The GST fusion proteins and GST were incubated with bacterial lysates containing flag tagged ICDI. In the last lane pure bacterial lysate containing ICDI was blotted. Binding was only observed to CT1.4-1610Stop. **B)** Expression of GST fusion proteins in bacteria. 25pmol were blotted (Δ EF: 47kDa, A: 46kDa). Expression of CT1.4-1610Stop see Figure 8E.

3.2.4 Abolishing CDI in $Ca_v1.2$ channels

To figure out whether the C-terminus of $Ca_v1.4\alpha1$ can abolish CDI in $Ca_v1.2$ channels, the whole C-terminus or parts of the C-terminus of $Ca_v1.2b\alpha1$ were replaced with the corresponding parts of $Ca_v1.4\alpha1$. A series of chimeric $\alpha1$ subunits was constructed (Figure 3-13A). Replacement of the whole cytosolic C-terminus of $Ca_v1.2b\alpha1$ with the C-terminus of $Ca_v1.4\alpha1$ (1.2-CT1.4) completely blocked CDI. Kinetics of I_{Ba} and I_{Ca} were not significantly different from each other and in the same range as for I_{Ca} of $Ca_v1.2$ wild type channels (Figure 3-13F, table 3-2). But no effect was seen when only the ICDI domain of $Ca_v1.4\alpha1$ was introduced in $Ca_v1.2b\alpha1$, replacing the last 149 amino acids (1.2-ICDI1.4). CDI was observed to the same extent as in $Ca_v1.2$ wild type channels with a f_{max} of about 0.3 and kinetic parameters not different from wild type channels (Figure 3-13F, table 3-2). As expected, CDI was completely blocked when the whole sequence downstream the IQ motif of $Ca_v1.2b\alpha1$ was exchanged with the corresponding sequence of $Ca_v1.4\alpha1$ (1.2-C+ICDI1.4). Normalized traces for I_{Ba} and I_{Ca} were completely congruent and kinetic parameters were again in the same range as for $Ca_v1.2$ (Figure 3-13B, table 3-2). The f value was not significantly different from zero over the whole voltage range with an f_{max} of 0.04 ± 0.03 (Figure 3-13C, F).

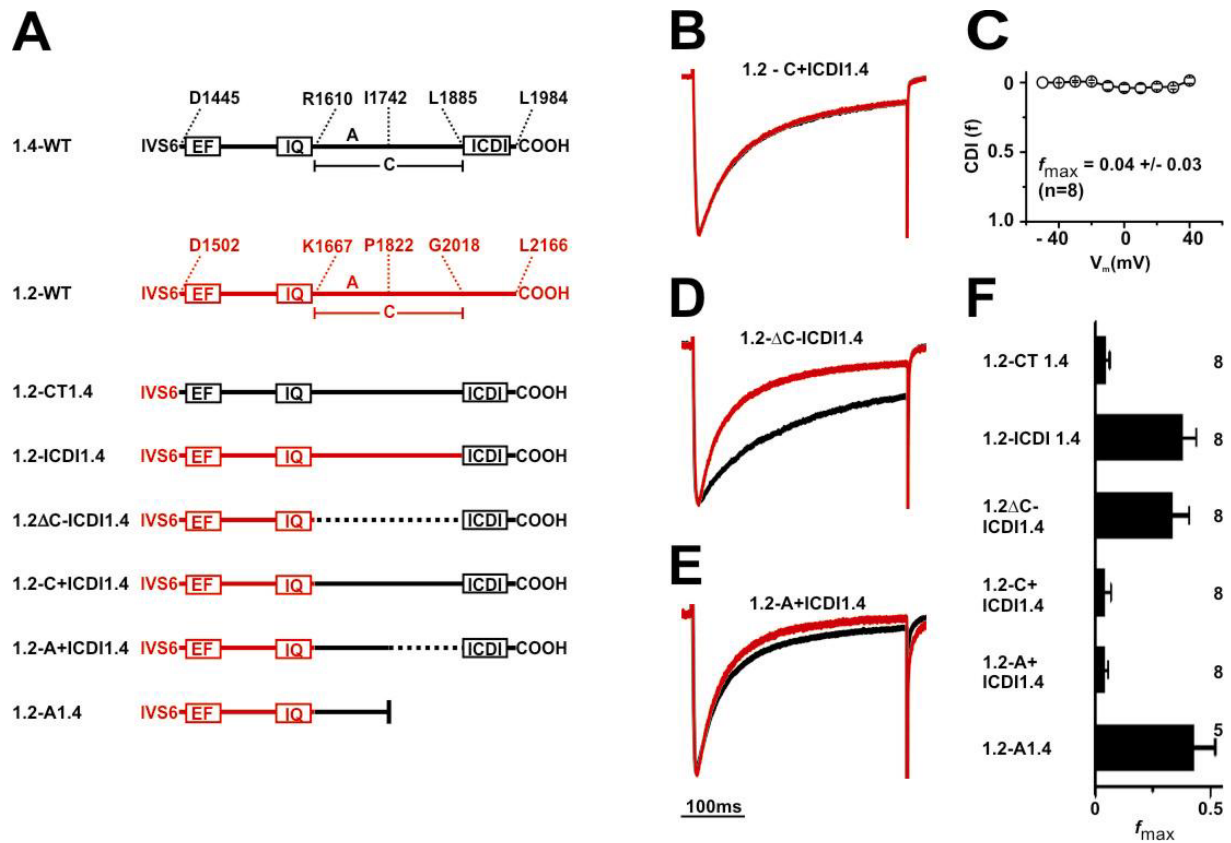


Figure 3-13 Abolishing CDI in chimeric $Ca_v1.4/Ca_v1.2$ channels. Currents were measured as mentioned in Figure 8. Kinetic parameters for all channels are given in table 3-2. **A**) Schematic representation of the C-terminus of $Ca_v1.4\alpha1$ (black) and $Ca_v1.2\beta\alpha1$ (red) and the constructed chimeras. **B**) Representative traces of I_{Ba} (black) and I_{Ca} (red) for chimera 1.2-C+ICDI1.4. **C**) Voltage dependence of f for 1.2-C+ICDI1.4. f_{max} is the maximum f value, n is the number of cells. No CDI was observed. **D**) Traces of I_{Ba} and I_{Ca} for 1.2ΔC-ICDI1.4. There is no difference to $Ca_v1.2$ wild type channels **E**) Traces of I_{Ba} and I_{Ca} for 1.2-A+ICDI1.4. CDI is completely blocked in this chimera. **F**) f_{max} values for the chimeric channels shown in A. Number of cells is indicated at the right side. Data for wild type channels see Figure 10.

Surprisingly, unlike in $Ca_v1.4$ channels the ICDI domain of $Ca_v1.4\alpha1$ was not able to block CDI in $Ca_v1.2$ channels when directly attached to the IQ motif of $Ca_v1.2\beta\alpha1$ (1.2ΔC-ICDI1.4). There was no difference to $Ca_v1.2$ wild type channels in both the f value and the kinetic parameters (Figure 3-13 D, F, table 3-2). To abolish CDI it was necessary to introduce at least peptide A and the ICDI domain of $Ca_v1.4\alpha1$ into the $Ca_v1.2\beta\alpha1$ subunit (1.2-A+ICDI1.4). For this chimera there was again no difference in I_{Ba} and I_{Ca} traces and kinetic parameters were in the range of those observed for I_{Ca} of wild type $Ca_v1.2$ channels. The f_{max} value was not significantly different from zero (Figure 3-13E, F, table 3-2). However, in the

absence of ICDI peptide A alone was not able to block CDI in Ca_v1.2 channels (1.2-A1.4). All parameters for this chimera were in the same range as for Ca_v1.2 wild type channels (Figure 3-13F, table 3-2). Unlike in Ca_v1.4 channels ICDI alone is not sufficient to block ICDI, it needs assistance of peptide A.

Table 3-2 Parameters for inactivation kinetics and f_{\max} values of wild type and mutant channels

| α_1 subunit coexpressed with β_2 and $\alpha_2\delta_1$ | charge carrier (mM) | τ_{fast} (ms) | τ_{slow} (ms) | A_{fast} (%) | n | f_{\max} | n |
|--|------------------------|---------------------------|---------------------------|-----------------------|----|---------------|----|
| Ca _v 1.4 | 10 Ca ²⁺ | n.i. | | | 10 | 0.01 ± 0.02 | 11 |
| | 10 Ba ²⁺ | n.i. | | | 10 | | |
| Ca _v 1.2b | 10 Ca ²⁺ | 42.6 ± 5.3 | 239.1 ± 28.4 | 61.3 ± 5.1 | 16 | 0.32 ± 0.05** | 11 |
| | 10 Ba ²⁺ | 238.4 ± 16.4 | | | 12 | | |
| C1884Stop | 10 Ca ²⁺ | 33.1 ± 5.9 | 168.7 ± 20.8 | 60.7 ± 6.1 | 13 | 0.30 ± 0.03** | 14 |
| | 10 Ba ²⁺ | n.i. | | | 13 | | |
| C1884Stop+CaM ₁₂₃₄ | 10 Ca ²⁺ | n.i. | | | 8 | 0.03 ± 0.02 | 8 |
| | 10 Ba ²⁺ | n.i. | | | 8 | | |
| C1884Stop+ICDI | 10 Ca ²⁺ | n.i. | | | 5 | 0.03 ± 0.03 | 5 |
| | 10 Ba ²⁺ | n.i. | | | 5 | | |
| 1.2-CT1.4 | 10 Ca ²⁺ | 20.5 ± 3.5 | 100.7 ± 16.1 | 73.5 ± 6.3 | 4 | 0.04 ± 0.02 | 8 |
| | 10 Ba ²⁺ | 26.9 ± 2.6 | 121.6 ± 12.1* | 63.1 ± 6.7 | 4 | | |
| 1.2-C+ICDI1.4 | 10 Ca ²⁺ | 40.1 ± 5.6 | 164.9 ± 28.5 | 57.5 ± 9.8 | 5 | 0.04 ± 0.03 | 8 |
| | 10 Ba ²⁺ | 43.4 ± 1.8 | 180.8 ± 20.1 | 51.0 ± 8.4 | 4 | | |
| 1.2-ICDI1.4 | 10 Ca ²⁺ | 39.5 ± 5.9 | 145.1 ± 11.0 | 62.5 ± 4.3 | 6 | 0.38 ± 0.06** | 8 |
| | 10 Ba ²⁺ | 182.8 ± 26.9 | | | 6 | | |
| 1.2ΔC-ICDI1.4 | 10 Ca ²⁺ | 49.2 ± 4.2 | 216.8 ± 23.3 | 50.0 ± 5.4 | 7 | 0.34 ± 0.07** | 8 |
| | 10 Ba ²⁺ | 239.5 ± 31.0 | | | 7 | | |
| 1.2-A+ICDI1.4 | 10 Ca ²⁺ | 29.9 ± 1.8 | 128.6 ± 25.0 | 58.7 ± 12.7 | 5 | 0.04 ± 0.01 | 8 |
| | 10 Ba ²⁺ | 25.3 ± 3.9 | 159.2 ± 35.2 | 47.3 ± 11.2 | 5 | | |

Inactivation parameters τ_1 , τ_2 and A_{fast} (%) for α_1 -subunits are indicated. Time course of inactivation of I_{Ba} of Ca_v1.2, 1.2-ICDI1.4 and 1.2ΔC-ICDI1.4 was fitted by a monoexponential function. For all other channels it was fitted with a biexponential function. n.i.: no inactivation as gauged by $r_{300} > 0.95$. r_{300} is the fraction of current remaining after 300ms depolarization. Statistical significance of kinetic parameters for I_{Ba} or I_{Ca} is given in comparison to those of I_{Ca} of Ca_v1.2. Statistical significance of f_{\max} is given in comparison to Ca_v1.4 wild type. Data are given as means ± SEM. Statistical differences were calculated by one-way ANOVA followed by Dunnett test (* $p < 0.05$, ** $p < 0.01$).

4 DISCUSSION

4.1 Functional characterization of $\text{Ca}_v1.4\alpha1$

The $\text{Ca}_v1.4\alpha1$ LTCC subunit is not able to form functional calcium channels on its own. The coexpression of β and $\alpha2\delta$ subunits is required to generate LTCC currents. This finding supports the notion that $\text{Ca}_v1.4$ calcium channels are heteromeric multisubunit complexes. As seen in our experiments $\text{Ca}_v1.4\alpha1$ can form LTCCs with different β subunits, but the current amplitudes were consistently bigger when coexpressed with $\beta2a$ subunit. One reason for this observation may be that $\text{Ca}_v1.4\alpha1$ binds to the $\beta2$ subunit with higher affinity than to the $\beta3$ subunit. This assumption is supported by studies showing that elimination of the $\beta3$ ⁶³ and $\beta4$ ⁶⁴ subunit in the mouse retina does not affect vision, whereas deletion of the $\beta2$ subunit results in a phenotype similar to CSNB2 in humans⁴⁵. Thus, in vitro and in vivo studies suggest that $\beta2$ is the native β subunit of $\text{Ca}_v1.4$ channels.

4.1.1 *Electrophysiological properties of $\text{Ca}_v1.4\alpha1$*

The electrophysiological profile of $\text{Ca}_v1.4\alpha1$ is unique among all LTCCs^{46,65,66}. Ba^{2+} currents passing $\text{Ca}_v1.4$ calcium channels activate with very fast kinetics, have a relatively low activation threshold compared to $\text{Ca}_v1.2$ channels and show an extreme slow inactivation time course. VDI of $\text{Ca}_v1.4$, which is an intrinsic property of the channel core^{14,15} and only depends on the membrane potential, is very slow. Up to 30s depolarization at V_{max} are needed for full inactivation of I_{Ba} . Due to this properties a so-called conductance window exists where the channel cycles between open and closed state without inactivating (Figure 4-1 and Figure 3-3 C). This conductance window is marked by the expanded overlapping region of activation and steady state inactivation curves of $\text{Ca}_v1.4$ channels (Figure 4-1, red). This feature enables the channel to provide a steady state inward current.

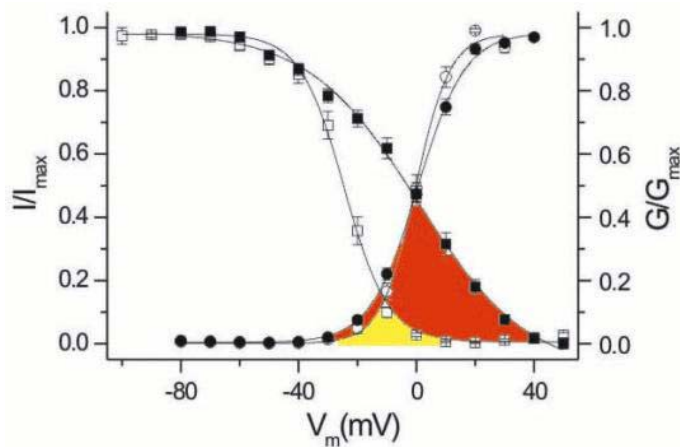


Figure 4-1 Conductance-voltage relationships for $\text{Ca}_v1.4$ (\bullet , $n = 28$) and $\text{Ca}_v1.2$ (\circ , $n = 9$) and steady state inactivation curves for $\text{Ca}_v1.4$ (\blacksquare , $n = 9$) and $\text{Ca}_v1.2$ (\square , $n = 9$). Individual curves were normalized to maximum current amplitude and then averaged. *Solid lines*: datafit to the Boltzmann equation (See Figure 3-3C). Red: conductance window for $\text{Ca}_v1.4\alpha1$. Yellow: overlapping area for $\text{Ca}_v1.2\beta\alpha1$.

4.1.2 Pharmacological profile of $\text{Ca}_v1.4\alpha1$

The pharmacological properties of $\text{Ca}_v1.4\alpha1$ are also different from the other LTCCs. Despite the fact that 12 of 13 amino acids required for high DHP sensitivity in $\text{Ca}_v1.2\beta\alpha1$ are conserved in the primary sequence of $\text{Ca}_v1.4\alpha1$ (Figure 1-4) the DHP sensitivity at -80mV is about 20-fold lower than for $\text{Ca}_v1.2\beta\alpha1$ ⁶⁷. The difference is a phenylalanine at position 1414 instead of a tyrosine at the corresponding position in $\text{Ca}_v1.2\beta\alpha1$. However, this small difference cannot be responsible for the low sensitivity. $\text{Ca}_v1.3\alpha1$ also exhibits low DHP sensitivity⁶⁸ but contains a tyrosine at the equivalent position, like $\text{Ca}_v1.2\beta\alpha1$ (Figure 1-4). Indeed, there could be other amino acids not yet identified that are important for the apparent affinity of DHPs, but it is very likely that the observed differences for $\text{Ca}_v1.4\alpha1$ in DHP binding result from its unique biophysical properties. The DHP block is highly voltage dependent^{69,70} because DHPs bind preferentially to the inactivated state of LTCCs. Due to the fact that $\text{Ca}_v1.4$ channels inactivate very slowly and show the mentioned conductance window in contrast to $\text{Ca}_v1.2$ channels, the affinity of DHPs to $\text{Ca}_v1.4\alpha1$ is decreased. This finding is corroborated by an experiment where the holding potential was shifted from -80mV to -50mV , increasing the fraction of channels in the inactivated state. In this experiment the DHP block was strongly increased. Also the low sensitivity of $\text{Ca}_v1.4$ currents to verapamil and diltiazem could be induced by the very specific inactivation properties of $\text{Ca}_v1.4\alpha1$.

Another surprising finding is that the IC_{50} of L-cis-diltiazem is in the same range than the IC_{50} of D-cis-diltiazem. In other LTCCs the affinity for L-cis-diltiazem is at least 20-fold lower than the affinity for D-cis-diltiazem^{13,62,71}. The binding site for diltiazem in $\text{Ca}_v1.2\beta\alpha1$ is overlapping with the binding site for DHPs⁷². Except for the tyrosine phenylalanine exchange

mentioned above the corresponding amino acids are completely conserved in Ca_v1.4α1. Hence, the different performance of Ca_v1.2b and Ca_v1.4 channels can not be explained at the moment. So far L-cis-diltiazem was thought to be a specific blocker for cyclic-nucleotide-gated (CNG) channels in rod and cone photoreceptors^{73,74}. These channels are required to depolarize photoreceptors in response to an increase of cGMP. In experiments micromolar concentrations of L-cis-diltiazem have been used to block these channels. In the light of our new findings extreme care has to be taken to distinguish the effects of the blocker on CNG channels from those on retinal Ca_v1.4 channels.

4.2 Proposed mechanism for block of CDI in Ca_v1.4 channels

Surprisingly, inactivation of Ca_v1.4 channels is not accelerated in the presence of Ca²⁺ as charge carrier compared to Ba²⁺ currents. Most HVA calcium channels have such a self-regulatory feedback mechanism to limit Ca²⁺ influx into the cell. Ca_v1.2b as a typical representative of LTCCs is strongly regulated by Ca²⁺. After passing the pore Ca²⁺ binds to calmodulin which is prebound to the cytosolic C-terminus of the channel. Thus it causes a very fast decay of I_{Ca} within milliseconds (CDI)^{16,26}.

The current view on CDI is that this process is conferred by the proximal C-terminus of the channel. In this study we extend this view to a domain residing in the proximal C-terminus of Ca_v1.4. The Ca²⁺ sensing apparatus of Ca_v1.2 resides in the proximal C-terminus of the channel^{17,21-28}. It consists of a sequence stretch (Pre-IQ and IQ motif) that binds calmodulin, the primary Ca²⁺ sensor and an EF hand motif. The EF hand is the transducing element between the Ca²⁺ sensing machinery and the inactivation gate of the channel. Although these sequences are highly conserved in Ca_v1.4α1 (Figure 6-1, alignment) and the whole HVA calcium channel family¹⁷⁻²⁹, Ca_v1.4 channels show no CDI (see alignment, Figure 6-1). The findings of this study exclude the loss of the Ca²⁺ sensor calmodulin as explanation for this behaviour. Despite the fact that binding of calmodulin to the C-terminus was only observed in the presence of Ca²⁺ in GST pull-down experiments, CaM₁₂₃₄, which corresponds to apocalmodulin, can bind to the C1884Stop mutant (Figure 3-10). Due to this fact apocalmodulin must be prebound to the channel like in Ca_v1.2

The data rather indicate that CDI is likely to be masked by an autoinhibitory channel domain. The ICDI domain (inhibitor of calcium dependent inactivation, L1885-L1984) was revealed as this channel domain and a stretch of 23 amino acids (Q1930-A1952) that is of outstanding importance for the block of CDI was identified within this domain in electrophysiological

experiments. Furthermore, it is shown that the ICDI domain interacts with the EF hand motif of the proximal C-terminus of LTCCs and coexpression experiments show (Figure 10E) that it acts as an independent protein unit that is sufficient for block of CDI in $Ca_v1.4$ channels. Considering primary structure analysis predicting an α -helical structure for the ICDI domain (predicted by PhD analysis⁷⁵, confidence level >82%) and the fact that the EF hand motif contains helices¹⁷, this two structures may form a paired helix complex with each other.

According to an established model, inactivation of HVA calcium channels is conferred by the so-called pore occluder (PO), which is formed by the cytoplasmatic I-II loop. This PO is a blocking particle that closes the pore¹⁴⁻¹⁶. When the channel is in the resting state the PO is tonically inhibited by the EF-hand³⁰. Changes in the membrane potential induce a slow conformational change and thus the inhibition of the PO by the EF hand is relieved. The PO now closes the pore with its intrinsic kinetics (VDI) (Figure 4-2A, top).

When Ca^{2+} passes the channel pore, it binds to apocalmodulin which is prebound to the proximal C-terminus. Subsequently, Ca^{2+} -calmodulin moves to its effector site and thereby induces a conformational change in the whole Ca^{2+} sensing apparatus. This results in a productive interaction between the EF hand and the PO that accelerates the movement of the PO (CDI) (Figure 4-2A, bottom)^{23,30}. This model is valid for wild type $Ca_v1.2$ channels and truncated $Ca_v1.4$ channels lacking the ICDI domain.

This study now extends the model to channels lacking CDI, like the retinal $Ca_v1.4$ LTCC and the $Ca_v1.2\beta\alpha1$ mutant carrying the distal C-terminus of $Ca_v1.4\alpha1$ (1.2-A+ICDI1.4; Figure 4-2B). In this channels the ICDI domain is permanently bound to the EF hand motif, which is a general downstream transduction element of CDI. Thus, the EF hand is uncoupled from the Ca^{2+} sensing machinery and there is no tonic inhibition of the PO and no acceleration of the PO movement in the presence of Ca^{2+} . CDI is abolished by the ICDI domain. Consequently, inactivation occurs strictly voltage dependent with kinetics intrinsic to the PO or rather the channel core. These intrinsic kinetics are very slow for $Ca_v1.4$ and fast for $Ca_v1.2$ channels. Theoretically, a mutant channel truncated immediately after the IVS6 transmembrane segment should show the intrinsic kinetic parameters of the channel core. We constructed such a mutant from $Ca_v1.4\alpha1$, G1458Stop. For an unknown reason no current could be measured from this channel.

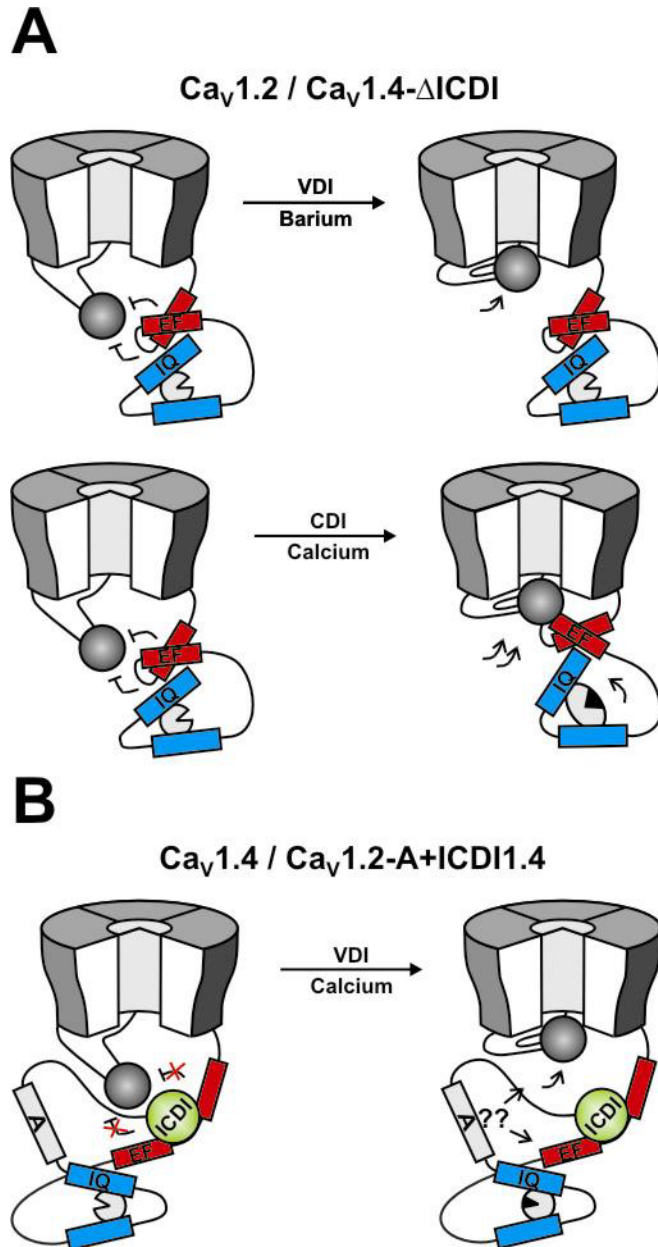


Figure 4-2 Model for CDI and VDI. **A, top)** In $\text{Ca}_v1.2$ wild type and $\text{Ca}_v1.4$ lacking ICDI voltage induces a slow conformational change that relieves tonic inhibition of the I-II loop (“pore occluder”, grey ball) by the EF motif and induces closure of the pore (VDI). **A, bottom)** Ca^{2+} binds to CaM and triggers an interaction of the EF hand with the pore occluder that speeds up channel closure, thus promoting fast CDI. **B)** In $\text{Ca}_v1.4$ and $\text{Ca}_v1.2$ carrying the distal C-terminus of $\text{Ca}_v1.4$ ICDI binds to the EF motif. Hence, the pore occluder is uncoupled from the EF hand and inactivation occurs in a voltage-dependent fashion with kinetics that are intrinsic to the respective channel core. The molecular target of peptide A remains to be determined.

This proposed mechanism is supported by the properties of a deletion mutant of $\text{Ca}_v1.2$ lacking the EF hand motif²³, which corresponds to our 1.2-A+ICDI1.4 chimera where the EF hand motif is disabled. This channel also shows no CDI and its inactivation time constants are nearly identical to the parameters of 1.2-A+ICDI1.4. Unfortunately, from the corresponding mutant of $\text{Ca}_v1.4\alpha1$ lacking the EF hand motif, $\text{Ca}_v1.4\Delta\text{EF}$, no measurable current was achieved. The molecular details of the interaction of peptide A in the $\text{Ca}_v1.2$ backbone are not known at the moment. We know that peptide A is not necessary to block CDI in $\text{Ca}_v1.4$ channels. By contrast, in $\text{Ca}_v1.2$ channels it is required but not sufficient to block CDI. Due to this findings it may support the inhibitory action of the ICDI domain via an indirect and

independent pathway. Since peptide A is not needed in $Ca_v1.4$ channels to abolish CDI, its contribution seems to be of minor importance. Attempts to narrow down the border of peptide A further more failed. It seems that the whole sequence is needed for blocking CDI.

4.3 Physiological function of $Ca_v1.4$ calcium channels

Our data show that the unique properties of retinal LTCC currents are caused by expression of $Ca_v1.4$ calcium channels. They are tailored to fulfill the tasks required in ribbon synapses of the retina. Ca^{2+} and Ba^{2+} currents obtained from native rod photoreceptor^{36,40,76} and bipolar cells^{39,77} show nearly the same properties as currents obtained from heterologously expressed $Ca_v1.4$ channels in HEK 293 cells (Figure 1-6). The only difference is that currents measured in native cells activate at 10-15mV more negative potentials^{36,39,40,76,78}. This difference may be explained by different environmental conditions and posttranslational modifications in native cells and HEK 293 cells. For the physiological function of the retina a tonic neurotransmitter release in the dark at the ribbon synapses of rod photoreceptor cells is essential. This glutamate release is triggered by a sustained Ca^{2+} inward current (Figure 4-3). Due to the very slow inactivation time course of $Ca_v1.4$ calcium currents, the conductance window and the lack of CDI, this channel is well suited to provide a sustained Ca^{2+} inward current into this cells over the required voltage range³⁹.

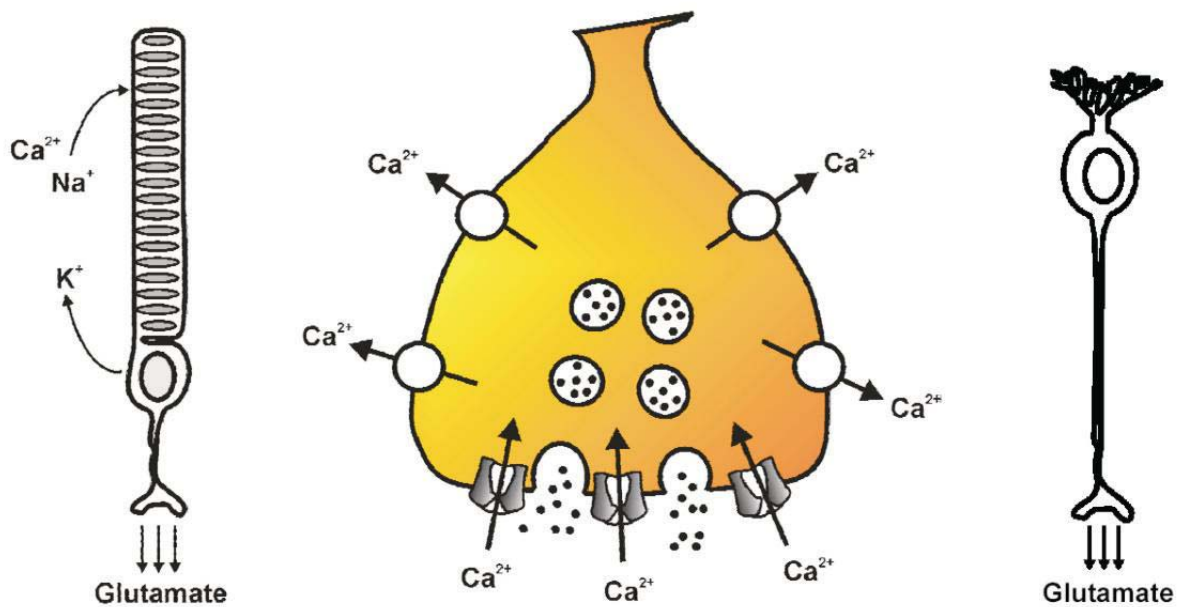


Figure 4-3 Schematic representation of a rod photoreceptor cell (left) and a bipolar cell (right). At the ribbon synapses of these cells a sustained Ca^{2+} influx mediates tonic neurotransmitter release (middle). $Ca_v1.4$ calcium channel currents, with its very slow time course of inactivation, are perfectly qualified to guarantee this sustained Ca^{2+} influx.

The properties of the heterologously expressed murine $Ca_v1.4$ calcium channel are consistent with the properties of its human counterpart⁶⁵. In humans different mutations in the gene coding for $Ca_v1.4\alpha1$ (CACNA1F) have been described. Several of the mutations lead to frame shifts or truncations within the channel core. Such massive exchanges almost surely will lead to the loss of function of the channel. The respective patients show the symptoms of CSNB2. Also an established mouse model with a loss of function mutation in the CACNA1F gene shows the same symptoms⁴². Interestingly, a few mutations in the human CACNA1F gene have been identified (K1591X and R1816X, corresponding to murine K1605X and R1834X)^{35,43} that do not affect the channel core. These mutations lead to truncations in the distal part of the C-terminus. The complete Ca^{2+} sensing apparatus will probably stay intact and only the ICDI domain is removed from the channel, according to our data. Even more interesting is the mutation 5665delC⁴⁴ that leads to a frame shift starting with residue 1888 (corresponding to murine S1895) and a premature stop after 43 unrelated amino acids. In this truncation mutant the $Ca_v1.4$ terminates immediately 10 aminoacids after the beginn of ICDI. All three truncations nearly correspond to truncation mutants presented in this study (Figure 6-2, alignment) and they also lead to CSNB2. How can this be explained? Maybe these mutations lead to aberrant folding of the proteins and thus to a complete loss of function. We cannot abandon this option completely. Our study provides an alternative model to explain this phenomenon. Considering our data these mutant channels will display CDI in contrast to wild type $Ca_v1.4$ channels. The mechansim of CDI is recovered and the sustained Ca^{2+} influx, which is essential for tonic neurotransmitter release at the ribbon synapses in the retina, is not existent anymore because the mutant channels inactivate. Retinal neurotransmission is impaired and, thus, we can explain the phenotype of these mutations.

5 SUMMARY

This study provides novel insights to the function and regulation of $\text{Ca}_v1.4$ LTCCs.

In the first part of the study the basic biophysical and pharmacological properties of $\text{Ca}_v1.4$ have been characterized. To this end $\text{Ca}_v1.4$ was cloned from murine retinal cDNA. The full-length cDNA comprises 6111bp and contains an open reading frame encoding for a protein of 1984 amino acids. $\text{Ca}_v1.4$ was functionally expressed in HEK 293 cells. Like in the case of other LTCCs the coexpression of $\alpha2\delta$ and β subunits was necessary to get measurable currents^{46,65,66}. The electrophysiological properties of $\text{Ca}_v1.4\alpha1$ found in patch clamp experiments distinguish these channels from other LTCCs. Activation kinetics were very fast, the activation threshold was relatively low and the time course of inactivation was extremely slow. Also the pharmacological properties were different from those of classical LTCCs. $\text{Ca}_v1.4$ channels show a much lower sensitivity for LTCC blockers compared to $\text{Ca}_v1.2b$ channels.

The most important findings of this study are the novel insights on the regulation of CDI. Surprisingly, no CDI was observed in $\text{Ca}_v1.4$ LTCCs in electrophysiological experiments. CDI is a negative feedback mechanism by which Ca^{2+} limits its own influx into the cell. This feedback inhibition is essential for many cell types to prevent excessive and potentially toxic Ca^{2+} levels and is widespread among HVA calcium channels. The sequences conferring CDI¹⁷⁻²⁹ are conserved throughout the whole HVA calcium channel family and also in $\text{Ca}_v1.4\alpha1$ raising the question of how this channel manages to switch off CDI. We identified an autoinhibitory domain in the distal C-terminus of $\text{Ca}_v1.4$ that serves to abolish CDI. This domain (ICDI, inhibitor of CDI) uncouples the molecular machinery conferring CDI from the inactivation gate by binding to the EF hand motif in the proximal C-terminus. Deletion of ICDI completely restores Ca^{2+} -calmodulin mediated CDI in $\text{Ca}_v1.4$. CDI can be switched off again in the truncated $\text{Ca}_v1.4$ channel by coexpression of ICDI indicating that it works as an autonomous unit. Furthermore, replacement of the distal C-terminus in the $\text{Ca}_v1.2b$ LTCC by the corresponding sequence of $\text{Ca}_v1.4$ is sufficient to block CDI. This finding suggests that autoinhibition of CDI can be principally introduced into other Ca^{2+} channel types.

The novel mechanism described is also of great physiological impact. In vivo, Ca_v1.4 is expressed in photoreceptors and bipolar cells of the retina. In these cells the lack of CDI is of great physiological importance since it is required to generate a sustained Ca²⁺ influx and, hence, to mediate tonic glutamate release from synaptic terminals^{38,79}. Mutations in the gene coding for the Ca_v1.4α1 subunit in humans are linked to a disease called congenital stationary nightblindness type 2 (CSNB2). Some of these mutations lead to truncated channels nearly identical to channel mutants analyzed in this study that show CDI. Thus, the phenotype of these mutations can be explained by the recovery of CDI.

6 APPENDIX

6.1 Sequence of Ca_v1.4 α 1 cloned from mouse retinal cDNA

1 ATGTCGGAATCTGAAGTCGGGAAAGATAACAACCCAGAGCCCAGTCCAGCCAATGGGACT
1 M S E S E V G K D T T P E P S P A N G T

61 GGCCTGGCCCTGAATGGGGCTCTGTCCTGGGCTCCAAGTGTGGGGACTGATACCAGC
21 G P G P E W G L C P G P P T V G T D T S

121 GGGCGTCAGGCCTGGGGACCCCAAGAAGAAGGACCCAGCACAACAAACACAAGACTGTG
41 G A S G L G T P R R R T Q H N K H K T V

181 GCGGTGGCCAGTGTCTCAGAGATCACCTCGAGCGCTCTTCTGCCTCACCCCTTACTAATCCC
61 A V A S A Q R S P R A L F C L T L T N P

241 ATTCGTCGGTCCTGCATCAGCATTGTAGAGTGAAGCCTTTTGATATTCTCATCCTCCTG
81 I R R S C I S I V E W K P F D I L I L L

IS1

301 ACAATCTTTGCCAACTGCGTGGCATTGGGGGTATATATCCCCTTCCCTGAGGACGACTCC
101 T I F A N C V A L G V Y I P F P E D D S

361 AACTGCTAACCACAACCTTGAACAGGTAGAATACGTGTTCCCTGGTGATTTTCACCGTG
121 N T A N H N L E Q V E Y V F L V I F T V

IS2

421 GAGACAGTGTCTCAAGATCGTAGCCTATGGGCTGGTGTCCATCCCAGCGCCTATATTTCG
141 E T V L K I V A Y G L V L H P S A Y I R

481 AATGGCTGGAACCTGCTCGACTTCATCATCGTCGTGGTCCGGGCTGTTCAGCGTGCTGCTG
161 N G W N L L D F I I V V V G L F S V L L

IS3

541 GAACAAGGACCTGGGCGGCCAGGAGATGCCCCGCATACTGGAGGAAAGCCAGGAGGCTTC
181 E Q G P G R P G D A P H T G G K P G G F

601 GATGTAAAGGCACTGCGGGCATTAGGGTGTACGACCTCTAAGGCTAGTGTCTGGGGT
201 D V K A L R A F R V L R P L R L V S G V

IS4

661 CCGAGTCTGCACATAGTGTCAATTCCATCATGAAGGCGCTTGTGCCGCTGCTGCACATT
221 P S L H I V L N S I M K A L V P L L H I

721 GCCCTGTTGGTGTCTTTCGTATTATCATTACGCCATCATCGGACTCGAGCTATTCCCTC
241 A L L V L F V I I I Y A I I G L E L F L

IS5

781 GGACGAATGCACAAGACATGCTACTTCTGGGATCTGATATGGAAGCAGAGGAGGACCCA
261 G R M H K T C Y F L G S D M E A E E D P

841 TCACCTTGTGCATCTTCTGGCTCTGGGCGTTCATGCACACTGAACCATAACCGAGTGCCGC
 281 S P C A S S G S G R S C T L N H T E C R

901 GGGCGCTGGCCAGGACCCAACGGTGGCATCACGAACTTCGACAATTTTTCTTTGCCATG
 301 G R W P G P N G G I T N F D N F F F A M

961 CTAAGTGTGTTCCAGTGTATTACCATGGAAGGCTGGACAGACGTCTCTACTGGATGCAG
 321 L T V F Q C I T M E G W T D V L Y W M Q

1021 ATGCCATGGGGTATGAGCTGCCTTGGGTGTACTIONTTGTGAGCCTTGTGCATCTTTGGGTCC
 341 D A M G Y E L P W V Y F V S L V I F G S

IS6

1081 TTCTTTGTCTCAACCTTGTGCTTGGAGTCCTAAGCGGGGAGTTCTCCAAGGAAAGAGAA
 361 F F V L N L V L G V L S G E F S K E R E

1141 AAGGCAAAAGCACGAGGTGACTTTTCAGAAGCTTCGGGAGAAGCAGCAGATGGAAGAAGAC
 381 K A K A R G D F Q K L R E K Q Q M E E D

1201 CTTCCGGGGCTACCTGGACTGGATCACACAGGCTGAGGAGTTAGACCTTCATGACCCCTCA
 401 L R G Y L D W I T Q A E E L D L H D P S

1261 GTAGACGGCAACTTGGCTTCTCTTGTCTGAAGAGGGACGGGCGGGCCATCGGCCACAACCTG
 421 V D G N L A S L A E E G R A G H R P Q L

1321 TCAGAGCTGACCAATAGGAGGCGCGGACGGCTGCGATGGTTCAGCCACTCTACTCGCTCC
 441 S E L T N R R R G R L R W F S H S T R S

1381 ACACACTCCACCAGCAGCCACGCCAGCCTCCCAGCCAGTGACACTGGCTCCATGACAGAC
 461 T H S T S S H A S L P A S D T G S M T D

1441 ACCCCTGGAGATGAGGATGAAGAAGAGGGGACCATGGCTAGCTGTACACGCTGCCTAAAC
 481 T P G D E D E E E G T M A S C T R C L N

1501 AAGATTATGAAAACAAGGATCTGCCGCCACTTCCGCCGAGCCAACCGGGGTCTCCGTGCA
 501 K I M K T R I C R H F R R A N R G L R A

1561 CGCTGCCGCCGGGCGTCAAGTCCAACGCCTGCTACTGGGCTGTACTGTTGCTCGTCTTC
 521 R C R R A V K S N A C Y W A V L L L V F

IIS1

1621 CTCAACACGTTGACCATAGCTTCAGAGCACCATGGGCAGCCTTTGTGGCTCACCCAGACC
 541 L N T L T I A S E H H G Q P L W L T Q T

1681 CAAGAGTATGCCAACAAAGTTCTGCTCTGCCTCTTCACTGTGGAGATGCTCCTCAAACCTG
 561 Q E Y A N K V L L C L F T V E M L L K L

IIS2

1741 TACGGCCTGGGCCCCTCTGTCTACGTTGCCTCCTTTTTCAACCGCTTTGACTGCTTCGTG
 581 Y G L G P S V Y V A S F F N R F D C F V

IIS3

1801 GTCTGTGGGGGCATCCTAGAAACCACTTTGGTGGAGGTGGGGGCCATGCAGCCTCTTGGC
 601 V C G G I L E T T L V E V G A M Q P L G

1861 ATCTCAGTGCTCCGATGTGTACGTCTCCTCAGGATCTTCAAGGTCACCAGGCACTGGGCA
 621 I S V L R C V R L L R I F K V T R H W A

IIS4

1921 TCCCTGAGCAATCTGGTGGCCTCTTTGCTCAATTCCATGAAGTCCATCGCCTCCTTGCTG
 641 S L S N L V A S L L N S M K S I A S L L

1981 CTTCTCCTCTTTCTCTTCATCATCATCTTCTCCCTGCTTGGCATGCAGCTGTTTGGGGC
 661 L L L F L F I I I F S L L G M Q L F G G

IIS5

2041 AAGTTCAACTTTGACCAGACCCACACCAAGAGGAGCACCTTTGATACCTTCCCCAAGCC
 681 K F N F D Q T H T K R S T F D T F P Q A

2101 CTCCTCACTGTCTTTTCAGATCCTGACTGGTGGAGGATTGGAACGTTGTCATGTATGATGGT
 701 L L T V F Q I L T G E D W N V V M Y D G

2161 ATCATGGCCTACGGTGGGCCCTTCTTCCCAGGGATGCTGGTGTGTGTTTATTTTCATCATC
 721 I M A Y G G P F F P G M L V C V Y F I I

IIS6

2221 CTCTTCATCTGTGGCAACTACATCCTGCTGAACGTGTTTCTTGCCATTGCCGTGGATAAC
 741 L F I C G N Y I L L N V F L A I A V D N

2281 CTAGCCAGCGGGGATGCAGGCACTGCCAAAGACAAGGGCAGAGAGAAGAGCAGTGAAGGA
 761 L A S G D A G T A K D K G R E K S S E G

2341 AACCTCCAAAGGAGAAACAAAGTATTGGTGCCTGGTGGAGAGAATGAGGACGCAAAGGGT
 781 N P P K E N K V L V P G G E N E D A K G

2401 GCAAGAAGTGAAGGAGCAGCACCAGGCATGGAGGAGGAGGAGGAGGAAGAAGAAGAA
 801 A R S E G A A P G M E E E E E E E E E

2461 GAGGAGGAGGAGGAAGAGGAAAATGGTGCAGGACATGTGGAACCTCTGCAGGAAGTAGTA
 821 E E E E E E E N G A G H V E L L Q E V V

2521 CCAAGGAGAAGGTGGTACCCATCCCTGAAGGCAGTGCCTTCTTCTGCCTTAGCCAAACC
 841 P K E K V V P I P E G S A F F C L S Q T

2581 AACCCGCTTCGGAAGGCCTGCCACACACTCATAACATCACCATATCTTACCAGTCTCATC
 861 N P L R K A C H T L I H H H I F T S L I

IIS1

2641 CTAGTGTTTCATCATCCTCAGTAGTGTGTCCCTGGCTGCTGAGGACCCCATCCGAGCTCAC
 881 L V F I I L S S V S L A A E D P I R A H

2701 TCCTTCCGAAACCATATTCTGGGATATTTTGATTATGCCTTACCTCCATATTCAGTGTG
 901 S F R N H I L G Y F D Y A F T S I F T V

IIS2

2761 GAGATTCTACTCAAGATGACAGTGTGGGGCCTTCCTGCACCGAGGCTCTTTCTGCCGT
 921 E I L L K M T V F G A F L H R G S F C R

2821 AGCTGGTTCAATCTGTTGGATCTCCTTGTGGTCAGTGTGTCCCTCATCTCCTTCGGCATC
 941 S W F N L L D L L V V S V S L I S F G I

III3

2881 CACTCCAGTGCCATCTCAGTTGTGAAGATTCTCCGAGTCCTCCGAGTCCTGCGGCCTCTC
 961 H S S A I S V V K I L R V L R V L R P L

III4

2941 CGAGCCATCAACAGAGCCAAGGGACTCAAGCATGTGGTGCAGTGTGTGTTTCGTGGCCATC
 981 R A I N R A K G L K H V V Q C V F V A I

3001 CGGACCATCGGAAACATCATGATTGTCACCACCCTCTTGCAGTTCATGTTTCGCCTGCATT
 1001 R T I G N I M I V T T L L Q F M F A C I

III5

3061 GGTGTTTCACTGTTCAAGGAAAATTCTACAGTTGCACCTGATGAGGCCAAACACACCCTG
 1021 G V Q L F K G K F Y S C T D E A K H T L

3121 AAAGAATGCAAGGGCTCCTTCCTCATCTACCCTGATGGAGATGTGTCACGACCTTTGGTC
 1041 K E C K G S F L I Y P D G D V S R P L V

3181 CGGGAGCGGCTCTGGGTCAACAGTGATTTTAACTTTGACAACGTCTTTCAGCCATGATG
 1061 R E R L W V N S D F N F D N V L S A M M

3241 GCCCTGTTCACTGTCTCTACCTTTGAAGGCTGGCCTGCGCTACTATACAAGGCCATAGAT
 1081 A L F T V S T F E G W P A L L Y K A I D

3301 GCAAACGCAGAAGATGAGGGCCCTATCTACAATTACCATGTGGAGATATCAGTATTCTTC
 1101 A N A E D E G P I Y N Y H V E I S V F F

III6

3361 ATTGTCTACATCATCATCGCCTTCTTCATGATGAACATCTTTGTGGGCTTTGTTATC
 1121 I V Y I I I I A F F M M N I F V G F V I

3421 ATCACATTCCGTGCCAGGGAGAGCAGGAGTACCAAACTGTGAACTGGACAAGAACCAG
 1141 I T F R A Q G E Q E Y Q N C E L D K N Q

3481 CGCCAGTGTGTGGAATATGCCCTCAAAGCTCAGCCACTCCGCCGATAACATCCCTAAGAAT
 1161 R Q C V E Y A L K A Q P L R R Y I P K N

3541 CCTCATCAGTACCGCGTGTGGGCCACTGTGAACTCTGCTGCCTTTGAGTACCTCATGTTT
 1181 P H Q Y R V W A T V N S A A F E Y L M F

IVS1

3601 CTGCTCATCCTGCTCAACACGGTGGCCCTAGCCATGCAGCACTATGAACAGACTGCTCCC
 1201 L L I L L N T V A L A M Q H Y E Q T A P

3661 TTTAACTATGCCATGGACATCCTCAACATGGTCTTCACTGGCCTCTTACCATTGAGATG
 1221 F N Y A M D I L N M V F T G L F T I E M

IVS2

3721 GTGCTCAAAATCATCGCCTTTAAACCCAAGCATTACTTTGCAGATGCCTGGAATACGTTT
 1241 V L K I I A F K P K H Y F A D A W N T F

IVS3

3781 GATGCTCTCATTGTAGTGGGCAGTGTAGTCGACATCGCCGTCACAGAAGTCAATAACGGA
 1261 D A L I V V G S V V D I A V T E V N N G

3841 GGCCATCTTGGCGAGAGTTCAGAGGACAGCTCCCGCATATCTATCACGTTCTTTTCGCCTC
 1281 G H L G E S S E D S S R I S I T F F R L

IVS4

3901 TTCCGAGTCATGAGGCTGGTCAAGCTTCTGAGTAAGGGTGAGGGGATCCGCACACTGCTC
 1301 F R V M R L V K L L S K G E G I R T L L

3961 TGGACATTCATCAAGTCTTCCAGGCCTTGCCCTATGTGGCACTTCTCATAGCAATGATA
 1321 W T F I K S F Q A L P Y V A L L I A M I

IVS5

4021 TTCTTCATCTATGCAGTCATTGGCATGCAGATGTTTGGCAAGGTGGCTCTTCAGGACGGC
 1341 F F I Y A V I G M Q M F G K V A L Q D G

4081 ACGCAGATAAATCGAAACAACAATTTCCAGACCTTTCCGCAGGCTGTGCTGCTTCTGTTC
 1361 T Q I N R N N N F Q T F P Q A V L L L F

4141 AGGTGTGCCACTGGTGAGGCCTGGCAAGAGATAATGCTAGCCAGCCTTCCAGGAAATCGA
 1381 R C A T G E A W Q E I M L A S L P G N R

4201 TGTGACCCTGAGTCTGACTTTGGCCCAGGCGAGGAATTTACCTGTGGTAGCAGTTTTGCC
 1401 C D P E S D F G P G E E F T C G S S F A

4261 ATCGTCTACTTCATCAGCTTCTTTATGCTCTGTGCCTTCTGATTATAAATCTCTTTGTG
 1421 I V Y F I S F F M L C A F L I I N L F V

IVS6

4321 GCTGTAATCATGGATAACTTTGATTACCTAACCAGAGATTGGTCTATCCTGGGACCCAC
 1441 A V I M D N F D Y L T R D W S I L G P H

4381 CACCTTGATGAATTCAAGAGGATCTGGTCTGAATATGACCCCGGAGCCAAGGGCCGCATC
 1461 H L D E F K R I W S E Y D P G A K G R I

4441 AAGCACTTGGATGTGGTTGCCCTGCTGAGACGCATCCAGCCCCATTGGGATTTGGAAG
 1481 K H L D V V A L L R R I Q P P L G F G K

4501 CTATGCCACACCGAGTGGCCTGCAAGAGACTCGTGGCAATGAATGTGCCCTCAACTCA
 1501 L C P H R V A C K R L V A M N V P L N S

4561 GATGGAACAGTGACATTCAACGCTACACTCTTTGCCCTGGTGC GGACATCCCTGAAGATC
 1521 D G T V T F N A T L F A L V R T S L K I

4621 AAGACAGAAGGGAACCTGGATCAAGCCAACCAGGAGCTTCGGATGGTCATCAAAAAGATC
 1541 K T E G N L D Q A N Q E L R M V I K K I

4681 TGGAAGCGGATAAAGCAGAAATTGTTGGATGAGGTCATCCCTCCTCCCGATGAGGAGGAG
1561 W K R I K Q K L L D E V I P P P D E E E

4741 GTCACTGTGGGAAAATTCTATGCCACATTCCTGATCCAAGATTATTTCCGAAAATTCCGG
1581 V T V G K F Y A T F L I Q D Y F R K F R

4801 AGAAGGAAAAGAAAAGGGGCTACTAGGAAGAGAGGCCCAACAAGCACATCCTCTGCCCTC
1601 R R K E K G L L G R E A P T S T S S A L

4861 CAGGCTGGTCTAAGGAGCCTGCAGGACTTGGGTCTGAGATCCGTCAAGCCCTCACCTAT
1621 Q A G L R S L Q D L G P E I R Q A L T Y

4921 GACACTGAGGAAGAAGAGGAAGAGGAAGAGGCAGTGGGTCAGGAGGCTGAGGAAGAGGAA
1641 D T E E E E E E E E A V G Q E A E E E E

4981 GCTGAGAACAACCCAGAACCATACAAAGACTCCATAGACTCCCAGCCCCAATCTCGATGG
1661 A E N N P E P Y K D S I D S Q P Q S R W

5041 AACTCTAGGATTTCCGGTGTCTCTACCTGTTAAGGAGAACTTCCAGATTCTCTCTCAACT
1681 N S R I S V S L P V K E K L P D S L S T

5101 GGGCCGAGTGATGATGATGGGCTGGCTCCCAACTCCAGGCAGCCCAGTGTGATACAGGCT
1701 G P S D D D G L A P N S R Q P S V I Q A

5161 GGCTCCCAACCACACAGGAGAAGCTCTGGGGTTTTTCATGTTCACTATCCCGGAAGAAGGA
1721 G S Q P H R R S S G V F M F T I P E E G

5221 AGTATTCAGCTCAAGGGA ACTCAAGGGCAGGACAATCAGAATGAGGAACAGGAAGTCCCT
1741 S I Q L K G T Q G Q D N Q N E E Q E V P

5281 GACTGGACTCCTGACCTGGATGAGCAGGCCGGGACTCCTTCGAACCCAGTCCTTTTACCA
1761 D W T P D L D E Q A G T P S N P V L L P

5341 CCTCACTGGTCCCAGCAACACGTAAACGGGCACCATGTGCCACGCCGACGTTTGCTGCCC
1781 P H W S Q Q H V N G H H V P R R R L L P

5401 CCCACGCCTGCAGGTCGGAAGCCCTCCTTCACCATCCAGTGTCTGCAACGCCAGGGCAGT
1801 P T P A G R K P S F T I Q C L Q R Q G S

5461 TGTGAAGATTTACCTATCCCAGGCACCTACCATCGTGGACGGACCTCAGGACCAAGCAGG
1821 C E D L P I P G T Y H R G R T S G P S R

5521 GCTCAGGGTTCCTGGGCAGCCCCTCCTCAGAAGGGTTCGACTGCTATATGCCCCCCTGTTG
1841 A Q G S W A A P P Q K G R L L Y A P L L

5581 TTGGTGGAGGAATCTACAGTGGGTGAAGGATACCTTGGCAA ACTTGGCGGCCCACTGCGT
1861 L V E E S T V G E G Y L G K L G G P L R

5641 ACCTTCACCTGTCTGCAAGTGCCTGGAGCTCATCCGAATCCCAGCCACCGCAAGAGGGGC
1881 T F T C L Q V P G A H P N P S H R K R G

5701 AGTGCTGACAGTTTGGTGGAGGCTGTGCTCATCTCCGAAGGCCTAGGTCTCTTTGCCCAA
1901 S A D S L V E A V L I S E G L G L F A Q

5761 GACCCACGATTTGTGGCCCTGGCCAAGCAGGAGATTGCAGATGCATGTCACCTGACCCTG
1921 D P R F V A L A K Q E I A D A C H L T L

5821 GATGAGATGGACAGTGCTGCCAGTGACCTGCTGGCACAGAGAACCACCTCCCTTTACAGT
1941 D E M D S A A S D L L A Q R T T S L Y S

5881 GATGAGGAGTCTATTCTTTCCCGCTTTGATGAAGAGGACCTGGGAGATGAGATGGCCTGT
1961 D E E S I L S R F D E E D L G D E M A C

5941 GTCCATGCCCTCTAA
1981 V H A L *

Bars below the lines indicate the transmembrane segments of the Cav1.4 α 1 subunit.

6.2 Alignment

| | | | | |
|--------|---|-------------|---------------|------|
| | | EF | Pre-IQ | |
| Cav1.2 | DNFDYLTRDWSILGPHHLDEFKRIWAEYDPEAKGRIKHLDVVLLLRRIQPPLGFGKLCPH | | | 1561 |
| Cav1.4 | DNFDYLTRDWSILGPHHLDEFKRIWSEYDFGAKGRIKHLDVVALLRRIQPPLGFGKLCPH | | | 1504 |
| <hr/> | | | | |
| Cav1.2 | RVACKRLVSMNPLNSDGTVMFNATLFAVVRTAIFIKTEGNIHQANEELRAI IKKIWKRT | | | 1621 |
| Cav1.4 | RVACKRLVAMNPLNSDGTVMFNATLFAVVRTSLKIKTEGNLDQANQELFM IKKIWKRI | | | 1564 |
| <hr/> | | | | |
| | | IQ | A | |
| Cav1.2 | SMKLLDQMPAGDDEVTVGKFYATFLIQEYFRKFKRKEQGLVGGKPSQRNALSLQAGI | | | 1680 |
| Cav1.4 | KQKLLDEVIPEDEEVTVGKFYATFLIQDYFRKFRKRRKEKGLLGRFAHTSTSSALQAGI | | | 1624 |
| | | ▲ | * | |
| <hr/> | | | | |
| Cav1.2 | RILHDIGPEIRRAISGDIIAEEFLDKAMKEAVSAASEDDIFRRAGLFGNHVSYVQSDSR | | | 1740 |
| Cav1.4 | RSIQDILGPEIROALTYDTEFEFEFEFEAVGQFAEFEFEAE.....NNPEPYKDSI | | | 1672 |
| | | | * | |
| <hr/> | | | | |
| Cav1.2 | SAFPQIFITQRPLHISKAGNNOGDTESSPSHEKIMDSITFTPSYSSTQSNANINNANNIAL | | | 1800 |
| Cav1.4 | DSQPQSRWNSR...ISVS.....LVREKLPDSISTGPSDDDGLAFNSRQPSVICA | | | 1720 |
| <hr/> | | | | |
| Cav1.2 | GRLFRPAGYFSTVSTVMEGHGSPSPAVRAQEAANKLSSKFCCHSCQESQIAMACQFCASQDD | | | 1860 |
| Cav1.4 | CSQPHRRSSCFMFTIFEESG.....IQLKGTQGDN.....QNEEQEVP | | | 1760 |
| <hr/> | | | | |
| Cav1.2 | NYDVRTIGEDAECCEPSSLISTEMLSYODDENRQIAPPEEEKRDIRLSPKKGFTIRASISIGR | | | 1920 |
| Cav1.4 | DWIPDIDECAGTESNFMVLLPFWHS..QOHVNGHVE.....RRRILPFTIPAGR | | | 1806 |
| | | | * | |
| <hr/> | | | | |
| Cav1.2 | RASFHIECLKROKNOGGDTSOKTVLFLFLMHHQALAVAGLSPLLQRSHSFTSIFRPCATIF | | | 1980 |
| Cav1.4 | KPSFTIQCLQRQ.....GSCEDLPTEGTMVHG.....FTSGPSRAQGSWAAP | | | 1848 |
| | | ▲ | | |
| <hr/> | | | | |
| | | ICDI | | |
| Cav1.2 | PATPGSRGWFFQPIFTLRLEGADSSSEKINSFSPSTHCGSWSGENSPCRGDSSAARRARPV | | | 2040 |
| Cav1.4 | ECKGRILYAPLLVVEESTVCEGYIKLGGELRTEITC..... | | | 1884 |
| | | * | | |
| <hr/> | | | | |
| Cav1.2 | SLIVPSCAGACGRQFHGSASSLVEAVLISEGLQFAQDPKFTIEVTIQEILADACDLTIEEM | | | 2100 |
| Cav1.4 | LQVPGAHPNFSHRKRGSADSLVEAVLISEGLGLFAQDHFVVALAKQEIADACHLITIDEM | | | 1943 |
| | | ▲ | * | |
| <hr/> | | | | |
| Cav1.2 | ENAADDIISGGARQSPNGTLLPFVNRDPGRDRAGQNEQDASGACAPGCGQSEEFALADR | | | 2159 |
| Cav1.4 | LSAASDILA.....QFTTSIYSDEE.....SILSRFDEEHLICDE | | | 1977 |
| | | * | | |
| <hr/> | | | | |
| Cav1.2 | RAGVSSI | | | 2166 |
| Cav1.4 | MACVHAL | | | 1984 |

Figure 6-1 Alignment of the C-termini of $Ca_v1.2\alpha1$ and $Ca_v1.4\alpha1$ starting at the end of the IVS6 segment. Bars on top of the lines indicate the borders of the EF hand motif, the Pre-IQ and the IQ segment, peptide A and the ICDI domain. Red asterisks indicate the amino acids mutated to stop codons in truncation mutants of $Ca_v1.4\alpha1$. Arrowheads indicate stop mutations observed in humans CSNB2^{35,43,44}. The arrowhead at S1895 indicates a frame shift leading to a premature stop after 43 unrelated amino acids

6.3 Primers

Table 6-1 Primers used for cloning of Ca_v1.4 α 1

| Primer Pair | Sequence (5' to 3') | Localization of Amplicon (AF192497) | Length of Amplicon (bp) |
|----------------|---|---|----------------------------|
| 17 | cggaattcgcgccaccATGTCGGAATCTGAAGTCGGGAA | nt 49-2138 | 2105 |
| 18 | GGTATCAAAGGTGCTCCTCTTGGT | | |
| 19 | CCATGAAGTCCATCGCCTCCTTG | nt 2003-4056 | 2054 |
| 20 | TGCCACATAGGGCAAGGCCTGGAA | | |
| 21 | G TTCAGAGGACACGTCCCGCATA | nt 3911-6006 | 2106 |
| 22 | gggtctcgagTTAGAGGGCATGGACACAG | | |

Coding sequences are represented in uppercase letters, 5'- and 3'-untranslated sequences are shown in lowercase letters.

7 REFERENCES

1. Catterall, W. A., Perez-Reyes, E., Snutch, T. P. & Striessnig, J. International Union of Pharmacology. XLVIII. Nomenclature and structure-function relationships of voltage-gated calcium channels. *Pharmacol Rev* **57**, 411-25 (2005).
2. Yu, F. H. & Catterall, W. A. The VGL-chanome: a protein superfamily specialized for electrical signaling and ionic homeostasis. *Sci STKE* **2004**, re15 (2004).
3. Takahashi, M., Seagar, M. J., Jones, J. F., Reber, B. F. & Catterall, W. A. Subunit structure of dihydropyridine-sensitive calcium channels from skeletal muscle. *Proc Natl Acad Sci U S A* **84**, 5478-82 (1987).
4. Hofmann, F., Biel, M. & Flockerzi, V. Molecular basis for Ca²⁺ channel diversity. *Annu Rev Neurosci* **17**, 399-418 (1994).
5. Lipscombe, D., Helton, T. D. & Xu, W. L-type calcium channels: the low down. *J Neurophysiol* **92**, 2633-41 (2004).
6. Koschak, A. et al. alpha 1D (Cav1.3) subunits can form l-type Ca²⁺ channels activating at negative voltages. *J Biol Chem* **276**, 22100-6 (2001).
7. Michna, M. et al. Cav1.3 (alpha1D) Ca²⁺ currents in neonatal outer hair cells of mice. *J Physiol* **553**, 747-58 (2003).
8. Safa, P., Boulter, J. & Hales, T. G. Functional properties of Cav1.3 (alpha1D) L-type Ca²⁺ channel splice variants expressed by rat brain and neuroendocrine GH3 cells. *J Biol Chem* **276**, 38727-37 (2001).
9. Scholze, A., Plant, T. D., Dolphin, A. C. & Nurnberg, B. Functional expression and characterization of a voltage-gated CaV1.3 (alpha1D) calcium channel subunit from an insulin-secreting cell line. *Mol Endocrinol* **15**, 1211-21 (2001).
10. Xu, W. & Lipscombe, D. Neuronal Ca(V)1.3alpha(1) L-type channels activate at relatively hyperpolarized membrane potentials and are incompletely inhibited by dihydropyridines. *J Neurosci* **21**, 5944-51 (2001).
11. Striessnig, J. Pharmacology, structure and function of cardiac L-type Ca(2+) channels. *Cell Physiol Biochem* **9**, 242-69 (1999).
12. Hofmann, F., Lacinova, L. & Klugbauer, N. Voltage-dependent calcium channels: from structure to function. *Rev Physiol Biochem Pharmacol* **139**, 33-87 (1999).
13. Hockerman, G. H., Peterson, B. Z., Johnson, B. D. & Catterall, W. A. Molecular determinants of drug binding and action on L-type calcium channels. *Annu Rev Pharmacol Toxicol* **37**, 361-96 (1997).
14. Stotz, S. C., Hamid, J., Spaetgens, R. L., Jarvis, S. E. & Zamponi, G. W. Fast inactivation of voltage-dependent calcium channels. A hinged-lid mechanism? *J Biol Chem* **275**, 24575-82 (2000).

15. Cens, T., Restituito, S., Galas, S. & Charnet, P. Voltage and calcium use the same molecular determinants to inactivate calcium channels. *J Biol Chem* **274**, 5483-90 (1999).
16. Bernatchez, G., Berrou, L., Benakezouh, Z., Ducay, J. & Parent, L. Role of Repeat I in the fast inactivation kinetics of the Ca(V)₂.3 channel. *Biochim Biophys Acta* **1514**, 217-29 (2001).
17. Erickson, M. G., Liang, H., Mori, M. X. & Yue, D. T. FRET two-hybrid mapping reveals function and location of L-type Ca²⁺ channel CaM preassociation. *Neuron* **39**, 97-107 (2003).
18. Liang, H. et al. Unified mechanisms of Ca²⁺ regulation across the Ca²⁺ channel family. *Neuron* **39**, 951-60 (2003).
19. DeMaria, C. D., Soong, T. W., Alseikhan, B. A., Alvania, R. S. & Yue, D. T. Calmodulin bifurcates the local Ca²⁺ signal that modulates P/Q-type Ca²⁺ channels. *Nature* **411**, 484-9 (2001).
20. Lee, A. et al. Ca²⁺/calmodulin binds to and modulates P/Q-type calcium channels. *Nature* **399**, 155-9 (1999).
21. Peterson, B. Z., DeMaria, C. D., Adelman, J. P. & Yue, D. T. Calmodulin is the Ca²⁺ sensor for Ca²⁺-dependent inactivation of L-type calcium channels. *Neuron* **22**, 549-58 (1999).
22. Qin, N., Olcese, R., Bransby, M., Lin, T. & Birnbaumer, L. Ca²⁺-induced inhibition of the cardiac Ca²⁺ channel depends on calmodulin. *Proc Natl Acad Sci U S A* **96**, 2435-8 (1999).
23. Zuhlke, R. D. & Reuter, H. Ca²⁺-sensitive inactivation of L-type Ca²⁺ channels depends on multiple cytoplasmic amino acid sequences of the alpha1C subunit. *Proc Natl Acad Sci U S A* **95**, 3287-94 (1998).
24. Zhou, J. et al. Feedback inhibition of Ca²⁺ channels by Ca²⁺ depends on a short sequence of the C terminus that does not include the Ca²⁺-binding function of a motif with similarity to Ca²⁺-binding domains. *Proc Natl Acad Sci U S A* **94**, 2301-5 (1997).
25. Zuhlke, R. D., Pitt, G. S., Deisseroth, K., Tsien, R. W. & Reuter, H. Calmodulin supports both inactivation and facilitation of L-type calcium channels. *Nature* **399**, 159-62 (1999).
26. Romanin, C. et al. Ca(2+) sensors of L-type Ca(2+) channel. *FEBS Lett* **487**, 301-6 (2000).
27. Pate, P. et al. Determinants for calmodulin binding on voltage-dependent Ca²⁺ channels. *J Biol Chem* **275**, 39786-92 (2000).
28. Pitt, G. S. et al. Molecular basis of calmodulin tethering and Ca²⁺-dependent inactivation of L-type Ca²⁺ channels. *J Biol Chem* **276**, 30794-802 (2001).

-
29. Halling, D. B., Aracena-Parks, P. & Hamilton, S. L. Regulation of voltage-gated Ca²⁺ channels by calmodulin. *Sci STKE* **2005**, re15 (2005).
 30. Kim, J., Ghosh, S., Nunziato, D. A. & Pitt, G. S. Identification of the components controlling inactivation of voltage-gated Ca²⁺ channels. *Neuron* **41**, 745-54 (2004).
 31. Chin, D. & Means, A. R. Calmodulin: a prototypical calcium sensor. *Trends Cell Biol* **10**, 322-8 (2000).
 32. Morgans, C. W. Localization of the alpha(1F) calcium channel subunit in the rat retina. *Invest Ophthalmol Vis Sci* **42**, 2414-8 (2001).
 33. Xu, H. P., Zhao, J. W. & Yang, X. L. Expression of voltage-dependent calcium channel subunits in the rat retina. *Neurosci Lett* **329**, 297-300 (2002).
 34. Bech-Hansen, N. T. et al. Loss-of-function mutations in a calcium-channel alpha1-subunit gene in Xp11.23 cause incomplete X-linked congenital stationary night blindness. *Nat Genet* **19**, 264-7 (1998).
 35. Strom, T. M. et al. An L-type calcium-channel gene mutated in incomplete X-linked congenital stationary night blindness. *Nat Genet* **19**, 260-3 (1998).
 36. Wilkinson, M. F. & Barnes, S. The dihydropyridine-sensitive calcium channel subtype in cone photoreceptors. *J Gen Physiol* **107**, 621-30 (1996).
 37. Rieke, F. & Schwartz, E. A. A cGMP-gated current can control exocytosis at cone synapses. *Neuron* **13**, 863-73 (1994).
 38. Schmitz, Y. & Witkovsky, P. Dependence of photoreceptor glutamate release on a dihydropyridine-sensitive calcium channel. *Neuroscience* **78**, 1209-16 (1997).
 39. Protti, D. A. & Llano, I. Calcium currents and calcium signaling in rod bipolar cells of rat retinal slices. *J Neurosci* **18**, 3715-24 (1998).
 40. Taylor, W. R. & Morgans, C. Localization and properties of voltage-gated calcium channels in cone photoreceptors of *Tupaia belangeri*. *Vis Neurosci* **15**, 541-52 (1998).
 41. Yagi, T. & Macleish, P. R. Ionic conductances of monkey solitary cone inner segments. *J Neurophysiol* **71**, 656-65 (1994).
 42. Mansergh, F. et al. Mutation of the calcium channel gene *Cacna1f* disrupts calcium signaling, synaptic transmission and cellular organization in mouse retina. *Hum Mol Genet* **14**, 3035-46 (2005).
 43. Wutz, K. et al. Thirty distinct CACNA1F mutations in 33 families with incomplete type of XLCSNB and *Cacna1f* expression profiling in mouse retina. *Eur J Hum Genet* **10**, 449-56 (2002).

-
44. Boycott, K. M. et al. A summary of 20 CACNA1F mutations identified in 36 families with incomplete X-linked congenital stationary night blindness, and characterization of splice variants. *Hum Genet* **108**, 91-7 (2001).
 45. Ball, S. L. et al. Role of the beta(2) subunit of voltage-dependent calcium channels in the retinal outer plexiform layer. *Invest Ophthalmol Vis Sci* **43**, 1595-603 (2002).
 46. Baumann, L., Gerstner, A., Zong, X., Biel, M. & Wahl-Schott, C. Functional characterization of the L-type Ca²⁺ channel Cav1.4alpha1 from mouse retina. *Invest Ophthalmol Vis Sci* **45**, 708-13 (2004).
 47. Biel, M. et al. Primary structure and functional expression of a high voltage-activated calcium channel from rabbit lung. *FEBS Lett* **269**, 409-12 (1990).
 48. Xia, X. M. et al. Mechanism of calcium gating in small-conductance calcium-activated potassium channels. *Nature* **395**, 503-7 (1998).
 49. Hullin, R. et al. Calcium channel beta subunit heterogeneity: functional expression of cloned cDNA from heart, aorta and brain. *Embo J* **11**, 885-90 (1992).
 50. Ellis, S. B. et al. Sequence and expression of mRNAs encoding the alpha 1 and alpha 2 subunits of a DHP-sensitive calcium channel. *Science* **241**, 1661-4 (1988).
 51. Kozak, M. Structural features in eukaryotic mRNAs that modulate the initiation of translation. *J Biol Chem* **266**, 19867-70 (1991).
 52. Birnboim, H. C. & Doly, J. A rapid alkaline extraction procedure for screening recombinant plasmid DNA. *Nucleic Acids Res* **7**, 1513-23 (1979).
 53. Graham, F. L., Smiley, J., Russell, W. C. & Nairn, R. Characteristics of a human cell line transformed by DNA from human adenovirus type 5. *J Gen Virol* **36**, 59-74 (1977).
 54. Graham, F. L. & van der Eb, A. J. A new technique for the assay of infectivity of human adenovirus 5 DNA. *Virology* **52**, 456-67 (1973).
 55. Ishiura, M. et al. Phage particle-mediated gene transfer to cultured mammalian cells. *Mol Cell Biol* **2**, 607-16 (1982).
 56. Bradford, M. M. A rapid and sensitive method for the quantitation of microgram quantities of protein utilizing the principle of protein-dye binding. *Anal Biochem* **72**, 248-54 (1976).
 57. Laemmli, U. K. Cleavage of structural proteins during the assembly of the head of bacteriophage T4. *Nature* **227**, 680-5 (1970).
 58. Mori, M. X., Erickson, M. G. & Yue, D. T. Functional stoichiometry and local enrichment of calmodulin interacting with Ca²⁺ channels. *Science* **304**, 432-5 (2004).

-
59. Naylor, M. J., Rancourt, D. E. & Bech-Hansen, N. T. Isolation and characterization of a calcium channel gene, *Cacna1f*, the murine orthologue of the gene for incomplete X-linked congenital stationary night blindness. *Genomics* **66**, 324-7 (2000).
 60. Berjukow, S. et al. Endogenous calcium channels in human embryonic kidney (HEK293) cells. *Br J Pharmacol* **118**, 748-54 (1996).
 61. Budde, T., Meuth, S. & Pape, H. C. Calcium-dependent inactivation of neuronal calcium channels. *Nat Rev Neurosci* **3**, 873-83 (2002).
 62. Glossmann, H., Linn, T., Rombusch, M. & Ferry, D. R. Temperature-dependent regulation of d-cis-[³H]diltiazem binding to Ca²⁺ channels by 1,4-dihydropyridine channel agonists and antagonists. *FEBS Lett* **160**, 226-32 (1983).
 63. Namkung, Y. et al. Targeted disruption of the Ca²⁺ channel beta3 subunit reduces N- and L-type Ca²⁺ channel activity and alters the voltage-dependent activation of P/Q-type Ca²⁺ channels in neurons. *Proc Natl Acad Sci U S A* **95**, 12010-5 (1998).
 64. Burgess, D. L., Jones, J. M., Meisler, M. H. & Noebels, J. L. Mutation of the Ca²⁺ channel beta subunit gene *Cchb4* is associated with ataxia and seizures in the lethargic (lh) mouse. *Cell* **88**, 385-92 (1997).
 65. Koschak, A. et al. Cav1.4alpha1 subunits can form slowly inactivating dihydropyridine-sensitive L-type Ca²⁺ channels lacking Ca²⁺-dependent inactivation. *J Neurosci* **23**, 6041-9 (2003).
 66. McRory, J. E. et al. The CACNA1F gene encodes an L-type calcium channel with unique biophysical properties and tissue distribution. *J Neurosci* **24**, 1707-18 (2004).
 67. Striessnig, J. et al. Structural basis of drug binding to L Ca²⁺ channels. *Trends Pharmacol Sci* **19**, 108-15 (1998).
 68. Xu, M., Welling, A., Papparisto, S., Hofmann, F. & Klugbauer, N. Enhanced expression of L-type Cav1.3 calcium channels in murine embryonic hearts from Cav1.2 deficient mice. *J Biol Chem* (2003).
 69. Kokubun, S., Prod'homme, B., Becker, C., Porzig, H. & Reuter, H. Studies on Ca channels in intact cardiac cells: voltage-dependent effects and cooperative interactions of dihydropyridine enantiomers. *Mol Pharmacol* **30**, 571-84 (1986).
 70. Kamp, T. J., Sanguinetti, M. C. & Miller, R. J. Voltage- and use-dependent modulation of cardiac calcium channels by the dihydropyridine (+)-202-791. *Circ Res* **64**, 338-51 (1989).
 71. Bohle, T. The effect of the benzothiazepine diltiazem on force and Ca²⁺ current in isolated frog skeletal muscle fibres. *J Physiol* **445**, 303-18 (1992).
 72. Hockerman, G. H., Dilmac, N., Scheuer, T. & Catterall, W. A. Molecular determinants of diltiazem block in domains IIIS6 and IVS6 of L-type Ca²⁺ channels. *Mol Pharmacol* **58**, 1264-70 (2000).

-
73. Kaupp, U. B. & Seifert, R. Cyclic nucleotide-gated ion channels. *Physiol Rev* **82**, 769-824 (2002).
 74. Finn, J. T., Grunwald, M. E. & Yau, K. W. Cyclic nucleotide-gated ion channels: an extended family with diverse functions. *Annu Rev Physiol* **58**, 395-426 (1996).
 75. Rost, B. & Sander, C. Prediction of protein secondary structure at better than 70% accuracy. *J Mol Biol* **232**, 584-99 (1993).
 76. Kourennyi, D. E. & Barnes, S. Depolarization-induced calcium channel facilitation in rod photoreceptors is independent of G proteins and phosphorylation. *J Neurophysiol* **84**, 133-8 (2000).
 77. von Gersdorff, H. & Matthews, G. Calcium-dependent inactivation of calcium current in synaptic terminals of retinal bipolar neurons. *J Neurosci* **16**, 115-22 (1996).
 78. Berntson, A., Taylor, W. R. & Morgans, C. W. Molecular identity, synaptic localization, and physiology of calcium channels in retinal bipolar cells. *J Neurosci Res* **71**, 146-51 (2003).
 79. Tachibana, M., Okada, T., Arimura, T., Kobayashi, K. & Piccolino, M. Dihydropyridine-sensitive calcium current mediates neurotransmitter release from bipolar cells of the goldfish retina. *J Neurosci* **13**, 2898-909 (1993).

8 PUBLICATIONS

Much B, Wahl-Schott C, Zong X, Schneider A, Baumann L, Moosmang S, Ludwig A, Biel M. Role of subunit heteromerization and N-linked glycosylation in the formation of functional hyperpolarization-activated cyclic nucleotide-gated channels. *J Biol Chem*. 2003 Oct 31;278(44):43781-6.

Baumann L, Gerstner A, Zong X, Biel M, Wahl-Schott C. Functional characterization of the L-type Ca²⁺ channel Cav1.4 α 1 from mouse retina. *Invest Ophthalmol Vis Sci*. 2004 Feb;45(2):708-13.

Wahl-Schott C, Baumann L, Zong X, Biel M. An arginine residue in the pore region is a key determinant of chloride dependence in cardiac pacemaker channels. *J Biol Chem*. 2005 Apr 8;280(14):13694-700.

Zong X, Eckert C, Yuan H, Wahl-Schott C, Abicht H, Fang L, Li R, Mistrik P, Gerstner A, Much B, Baumann L, Michalakakis S, Zeng R, Chen Z, Biel M. A novel mechanism of modulation of hyperpolarization-activated cyclic nucleotide-gated channels by Src kinase. *J Biol Chem*. 2005 Oct 7;280(40):34224-32.

Wahl-Schott C*, Baumann L*, Cuny H, Eckert C, Biel M. Switching off calcium dependent inactivation in L-type calcium channels by an autoinhibitory domain. Manuscript submitted.

9 ACKNOWLEDGEMENTS

Bei Herrn Prof. Dr. Martin Biel bedanke ich mich herzlich für die Aufnahme in seine Arbeitsgruppe, die Betreuung der Arbeit und die stets offene Tür für Probleme und Fragen.

Mein Dank gilt außerdem Herrn Prof. Dr. Alexander Pfeifer für die Übernahme des Koreferats.

Herrn Dr. Christian Wahl-Schott danke ich für die Betreuung und die zahlreichen anregenden Diskussionen während meiner Arbeit. Besonders bedanken möchte ich mich für die fundierte Einarbeitung in die Elektrophysiologie. Gerade am Anfang meiner Arbeit wäre ein Vorankommen ohne seine Hilfe viel schwieriger gewesen.

In diesem Zusammenhang danke ich auch Herrn PD Dr. Xiangang Zong für zahlreiche anregende Diskussionen während meiner Arbeit.

Mein besonderer Dank geht an Hartmut Cuny, Melanie Gebhard und vor allem auch an Christian Eckert. Sie haben mich im Labor immer tatkräftig unterstützt. Ohne sie hätte die Arbeit wohl etwas länger gedauert.

Für die gewissenhafte Durchsicht der Arbeit bedanke ich mich ganz herzlich bei Heidi und Christian.

Für den meist sehr angenehmen und häufig lustigen Laboralltag danke ich sämtlichen Mitgliedern unseres Arbeitskreises sehr herzlich. Ich bedanke mich an dieser Stelle auch für die eine oder andere mehr oder weniger feucht-fröhliche Feierabendrunde.

10 CURRICULUM VITAE

Persönliche Daten:

Name: Ludwig Alois Baumann
Anschrift: Jakob-Klar-Str. 10
80796 München

Geburtsdatum, -ort: 25. September 1975, Eichendorf
Staatsangehörigkeit: deutsch

Schule, Zivildienst, Studium:

09/86 – 05/95 **Schulausbildung**
Gymnasium Landau an der Isar
Naturwissenschaftlicher Zweig

08/95 – 08/96 **Zivildienst**

11/96 – 03/01 **Studium der Pharmazie**
Universität Regensburg

08/98 **1. Staatsexamen**

03/01 **2. Staatsexamen**

Praktische Ausbildung:

05/01 – 10/01 **Arcis Apotheke, München**

11/01 – 04/02 **Apotheke des Bezirkskrankenhauses Haar**

06/02 **3. Staatsexamen**

02/03 Erteilung der **Approbation als Apotheker**
der Bayerischen Landesapothekerkammer (BLAK)

Beruflicher Werdegang:

07/02 – 05/06 **Wissenschaftlicher Mitarbeiter/Doktorand**
Ludwig Maximilians Universität, München
Department Pharmazie
Lehrstuhl Pharmakologie für Naturwissenschaften
Prof. Dr. Martin Biel